Electronic Supplementary Material (ESI) for New Journal of Chemistry.
This journal is © The Royal Society of Chemistry and the Centre National de la Recherche Scientifique 2020

Electronic Supplementary Information

Fluorine-induced emission enhancement of tolanes via formation of tight molecular aggregates

Masato Morita, Shigeyuki Yamada,* and Tsutomu Konno

Faculty of Molecular Chemistry and Engineering, Kyoto Institute of Technology, Matsugasaki, Sakyo-ku, Kyoto 606-8585, Japan.

E-mail: syamada@kit.ac.jp

1. Experimental section

1-1. Measurement and characterization ••• **S-3**

1-1-1. General method

1-1-2. Photophysical properties

1-1-3. Single crystal X-ray diffraction

1-1-4. DFT calculation

1-2. Materials

General procedure for Sonogashira cross-coupling reaction

1-methoxy-4-[2-(4-methoxyphenyl)ethyn-1-yl]benzene (**1a**) ••• **S-4**

1-trifluoromethyl-4-[2-(4-methoxyphenyl)ethyn-1-yl]benzene (**1b**) ••• **S-4**

1-cyano-4-[2-(4-methoxyphenyl)ethyn-1-yl]benzene (**1c**) ••• **S-5**

1,2,4,5-Pentafluoro-3-methoxy-6-[2-(4-methoxyphenyl)ethyn-1-yl]benzene (**2a**) ••• **S-5**

General procedure for aromatic nucleophilic substitution

1,2,4,5-Pentafluoro-3-trifluoromethyl-6-[2-(4-methoxyphenyl)ethyn-1-yl]benzene (**2b**) ••• **S-6**

1,2,4,5-Pentafluoro-3-cyano-6-[2-(4-methoxyphenyl)ethyn-1-yl]benzene (**2c**) ••• **S-6**

NMR spectra of 1a–c and 2a–c ••• **S7~16**

2. Figure and Table ••• S17~24

3. Geometry optimization ••• S25~30

3-1. Geometry optimization for **1a**

3-2. Geometry optimization for **1b**

3-3. Geometry optimization for **1c**

3-4. Geometry optimization for **2a**

3-5. Geometry optimization for **2b**

3-6. Geometry optimization for **2c**

4. References ••• S31

1. Experimental section

1-1. Measurement and characterization

1-1-1. General method

^{1}H and ^{13}C NMR spectra were obtained with a Bruker AVANCE III 400 NMR spectrometer (^{1}H: 400 MHz and ^{13}C: 100 MHz) in chloroform-*d* ($CDCl_3$) solution and the chemical shifts are reported in parts per million (ppm) using the residual proton in the NMR solvent. ^{19}F NMR (376 MHz) spectra were obtained with a Bruker AVANCE III 400 NMR spectrometer in $CDCl_3$ solution with $CFCl_3$ (δ_F = 0 ppm) as an internal standard. Infrared (IR) spectra were recorded in a KBr method with a JASCO FT/IR-4100 type A spectrometer; all spectra were reported in wavenumber (cm^{-1}). High resolution mass spectra (HRMS) were recorded on a JEOL JMS700MS spectrometer using fast atom bombardment (FAB) methods. All chemicals including solvent were of reagent grade and where necessary were purified in the usual manner prior to use. Column chromatography was carried out on silica gel (Wakogel® 60N, 38–100 μm) and thin-layer chromatography (TLC) analysis was performed on silica gel TLC plates (Merck, Silica gel $60F_{254}$).

1-1-2. Photophysical properties

UV-vis absorption spectra were recorded on a JASCO V-500 absorption spectrometer. Steady-state PL spectra in solution and in crystal, and quantum yields were acquired using a JASCO FP-6600 fluorescence spectrometer or an absolute PL quantum yield measurement system (Quantaurus-QY, Hamamatsu Photonics, C11347-01) with a calibrated integrating sphere. PL lifetime (τ) was obtained using a Quantaurus-Tau Fluorescence lifetime spectrometer (Hamamtsu Photonics, C11367-34).

1-1-3. Single crystal X-ray diffraction

XRD spectra were recorded on a Rigaku XtaLAB AFC11 diffractometer (Rigaku Corporation, Tokyo, Japan). The reflection data were integrated, scaled, and averaged using CrysAlisPro (ver. 1.171.39.43a, Rigaku Oxford Diffraction, 2015). Empirical absorption corrections were applied using the SCALE 3 ABSPACK scaling algorithm (CrysAlisPro). Structures were solved by a direct method (SHELXT-2018/2) and refined using a full-matrix least square method (SHELXL-2018/3) visualized by Olex2-1.3[1,2].

1-1-4. DFT calculation

All computations were carried out using density functional theory (DFT) with the Gaussian 16 (Rev. B.01)[3] package. Geometry optimizations were executed using the M06-2X hybrid functional and 6-31+G(d) basis set with a CPCM[4] for heptane. Vertical excitations were also calculated using a TD-DFT method at the same level of theory.

1-2. Materials

General procedure for Sonogashira cross-coupling reaction

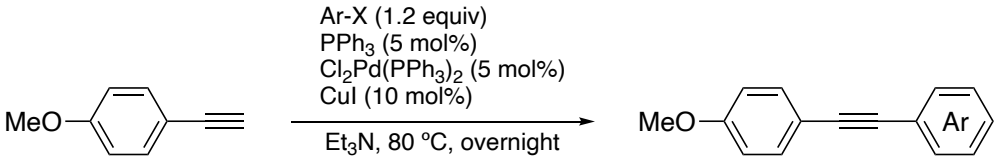

1a: 81%, **1b**: 68%, **1c**: 64%, **2a**: 40%

In a flask were placed an aromatic halide (Ar-X), 4-ethynylanisole, $Cl_2Pd(PPh_3)_2$, PPh_3, CuI, and Et_3N, and the suspended solution was stirred at 80 ºC temperature overnight. After the reaction time indicated, precipitate formed during reaction was separated by atmospheric filtration, and the filtrate was poured into saturated aqueous NH_4Cl solution. Crude product was extracted with AcOEt (three times) and the organic layer combined was washed with brine (once). Organic layer collected was dried over anhydrous Na_2SO_4, which was separated by filtrated. The filtrate was evaporated *in vacuo* and subjected to silica-gel column chromatography to obtain the desired product.

1-Methoxy-4-[2-(4-methoxyphenyl)ethyn-1-yl]benzene (1a)

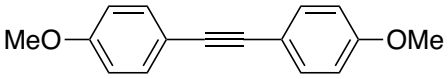

Sonogashira cross-coupling reaction was carried out using 4-iodoanisole (1.174 g, 5.00 mmol), 4-ethynylanisole (0.794 g, 6.00 mmol), $Cl_2Pd(PPh_3)_2$ (0.169 g, 0.25 mmol), PPh_3 (0.096 g, 0.25 mmol), CuI (0.100 g, 0.50 mmol) in Et_3N (25 mL), according to the general procedure. Purification by column chromatography (hexane : EtOAc = 10 : 1) afforded compound **1a** (0.97 g, 4.1 mmol, 81% yield, white solid). Single crystal was obtained by recrystallization from CH_2Cl_2/MeOH. m.p. = 155.7–157.1 ºC. ^{1}H NMR ($CDCl_3$): δ 3.83 (s, 6H), 6.85–6.89 (m, 2H), 7.43–7.47 (m, 2H); ^{13}C NMR ($CDCl_3$): δ 55.37, 88.06, 114.06, 115.80, 132.97, 159.48; IR (KBr): ν 3018, 2967, 2936, 2841, 2371, 2360, 2043, 1607, 1509, 1243, 1171, 1026, 836 cm^{-1}; HRMS (FAB+) *m/z* $[M]^+$ calcd for $C_{16}H_{14}O_2$: 238.0994; found: 238.0994.

1-Trifluoromethyl-4-[2-(4-methoxyphenyl)ethyn-1-yl]benzene (1b)

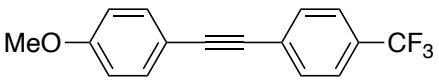

Sonogashira cross-coupling reaction was carried out using 4-bromotrifluoromethylbenzene (1.357 g, 6.00 mmol), 4-ethynylanisole (0.669 g, 5.00 mmol), $Cl_2Pd(PPh_3)_2$ (0.190 g, 0.25 mmol), PPh_3 (0.087 g, 0.25 mmol), CuI (0.075 g, 0.50 mmol) in Et_3N (25 mL), according to the general procedure. Purification by column chromatography (hexane : EtOAc = 20 : 1) afforded compound **1b** (0.91 g, 3.4 mmol, 68% yield, white solid). Single crystal was obtained by recrystallization from CH_2Cl_2/MeOH. m.p. = 125.5–127.2 ºC. ^{1}H NMR ($CDCl_3$): δ 3.84 (s, 3H), 6.88–6.92 (m, 2H), 7.47–7.51 (m, 2H), 7.60 (s, 4H); ^{13}C NMR ($CDCl_3$): δ 55.41, 86.98, 92.09, 114.25, 114.76, 124.16 (q, J = 270.3 Hz), 125.35 (q, J = 3.7 Hz) 127.16, 129.66 (q, J = 32.7 Hz), 131.73, 133.40, 160.22; ^{19}F NMR ($CDCl_3$): δ –63.22 (s, 3F); IR (KBr): ν 3029, 2970, 2940, 2845, 2218, 2170, 1928, 1604, 1521, 1465, 1326, 1102, 845 cm^{-1}; HRMS (FAB+) *m/z* $[M]^+$ calcd for $C_{16}H_{11}F_3O$: 276.0762; found: 276.0770.

1-Cyano-4-[2-(4-methoxyphenyl)ethyn-1-yl]benzene (1c)

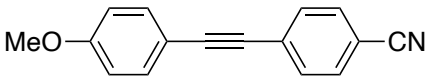

Sonogashira cross-coupling reaction was carried out using 4-bromobenzonitrile (1.098 g, 6.00 mmol), 4-ethynylanisole (0.683 g, 5.00 mmol), $Cl_2Pd(PPh_3)_2$ (0.165 g, 0.25 mmol), PPh_3 (0.068 g, 0.25 mmol), CuI (0.072 g, 0.50 mmol) in Et_3N (25 mL), according to the general procedure. Purification by column chromatography (hexane : EtOAc = 7 : 1) afforded compound **1c** (0.88 g, 3.2 mmol, 64% yield, white solid). Single crystal was obtained by recrystallization from CH_2Cl_2/MeOH. m.p. = 124.5–125.3 ºC. ^{1}H NMR ($CDCl_3$): δ 3.84 (s, 3H), 6.88–6.92 (m, 2H), 7.47–7.50 (m, 2H), 7.56–7.63 (m, 4H); ^{13}C NMR ($CDCl_3$): δ 55.46, 86.84, 94.21, 111.12, 114.28, 114.35, 118.75, 128.74, 131.95, 132.12, 133.47, 160.39; IR (KBr): ν 3087, 2971, 2945, 2846, 2225, 2211, 1597, 1509, 1291, 1251, 1026, 835 cm^{-1}; HRMS (FAB+) *m/z* $[M]^+$ calcd for $C_{16}H_{11}NO$: 233.0841; found: 233.0848.

1,2,4,5-Tetrafluoro-3-methoxy-6-[2-(4-methoxyphenyl)ethyn-1-yl]benzene (2a)

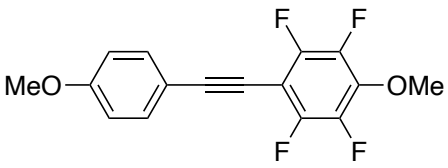

Sonogashira cross-coupling reaction was carried out using 4-bromo-2,3,5,6-tetrafluoroanisole (1.178 g, 4.20 mmol), 4-ethynylanisole (0.463 g, 3.50 mmol), $Cl_2Pd(PPh_3)_2$ (0.153 g, 0.18 mmol), PPh_3 (0.049 g, 0.18 mmol), CuI (0.067 g, 0.35 mmol) in Et_3N (15 mL), according to the general procedure. Purification by column chromatography (hexane : EtOAc = 20 : 1) afforded compound **2a** (0.44 g, 1.4 mmol, 40% yield, white solid). Single crystal was obtained by recrystallization from CH_2Cl_2/MeOH. m.p. = 116.3–117.0 ºC. ^{1}H NMR ($CDCl_3$): δ 3.84 (s, 3H), 4.11 (t, *J* = 1.5 Hz), 6.88–6.91 (m, 2H), 7.49–7.53 (m, 2H); ^{13}C NMR ($CDCl_3$): δ 55.51, 62.36 (t, *J* = 4.0 Hz), 73.04 (t, *J* = 3.5 Hz), 98.63 (t, *J* = 18.0 Hz), 100.65 (t, *J* = 3.5 Hz), 114.21, 114.27, 133.55, 138.61 (ddd, *J* = 15.0, 12.0, 3.0 Hz), 140.94 (ddt, *J* = 245.0, 15.0, 4.5 Hz), 147.31 (dm, *J* = 249.0 Hz), 160.58; ^{19}F NMR ($CDCl_3$): δ –158.82 (dd, *J* = 18.8, 7.5 Hz, 2F), –138.77 (dd, *J* = 22.6, 7.5 Hz, 2F); IR (KBr): ν 2962, 2935, 2842, 2368, 2360, 2213, 1604, 1520, 1491, 1427, 1248, 984, 831 cm^{-1}; HRMS (FAB+) m/z $[M]^+$ calcd for $C_{16}H_{10}F_4O_2$: 310.0617; found: 310.0630.

General procedure for aromatic nucleophilic substitution via lithium acetylide

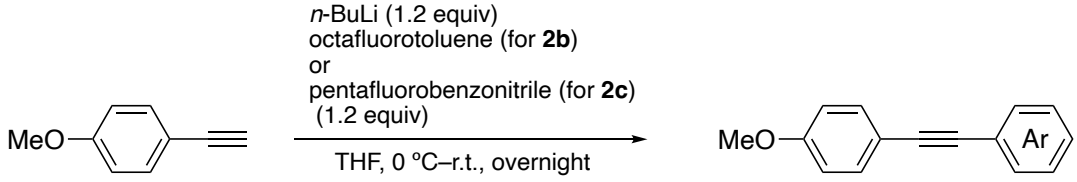

2b: 64%, **2c**: 40%

In a two-necked round bottomed flask, equipped with a teflon-coated stirring bar, was placed 4-ethynylanisole and THF, and cooled to 0 ºC. To the solution was added a solution of *n*-BuLi. After stirring at 0 ºC for 30 min, to the solution was added octafluorotoluene or pentafluorobenzonitrile at 0 ºC. After stirring at room temperature overnight, the mixture was poured into saturated NH_4Cl solution and the crude product was extracted with CH_2Cl_2 (three times) and organic layer combined was washed with

brine (once). Organic layer collected was dried over anhydrous Na_2SO_4, which was separated by filtration. The filtrate was evaporated *in vacuo* and subjected to silica-gel column chromatography to obtain the desired product.

1,2,4,5-Tetrafluoro-3-trifluoromethyl-6-[2-(4-methoxyphenyl)ethyn-1-yl]benzene (2b)

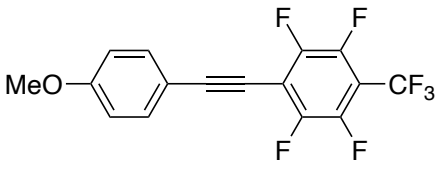

Aromatic nucleophilic substitution was carried out using octafluorotoluene (0.85 mL, 6.00 mmol), 4-ethynylanisole (0.67 g, 5.00 mmol), *n*-BuLi (1.6 M in hexane) (3.8 mL, 6.0 mmol) in THF (20 mL), according to the general procedure. Purification by column chromatography (hexane : EtOAc = 20 : 1) afforded compound **2b** (1.12 g, 3.2 mmol, 64% yield, white solid). Single crystal was obtained by recrystallization from CH_2Cl_2/MeOH. m.p. = 93.0–93.7 ºC. ^{1}H NMR ($CDCl_3$): δ 3.86 (s, 3H), 6.91–6.94 (m, 2H), 7.53–7.57 (m, 2H); ^{13}C NMR ($CDCl_3$): δ 55.53, 72.64 (t, J = 8.0 Hz), 105.63 (t, J = 7.0 Hz), 108.15–109.45 (m), 109.62 (t, J = 17.0 Hz), 113.16, 114.44, 120.97 (q, J = 276 Hz), 134.01, 144.26 (dm, J = 261 Hz), 146.86 (dm, J = 252 Hz), 161.32; ^{19}F NMR ($CDCl_3$): δ –56.62 (t, J = 41.4 Hz, 3F), –135.67 (ddd, J = 18.8, 16.9, 3.8, 2F), –141.69 (m, 2F); IR (KBr): ν 2969, 2945, 2919, 2847, 2548, 2363, 2224, 1901, 1647, 1604, 1496, 1182, 984, 837 cm^{-1}; HRMS (FAB+) *m/z* $[M]^+$ calcd for $C_{16}H_7F_7O$: 348.0385; found: 348.0390.

1,2,4,5-Pentafluoro-3-cyano-6-[2-(4-methoxyphenyl)ethyn-1-yl]benzene (2c)

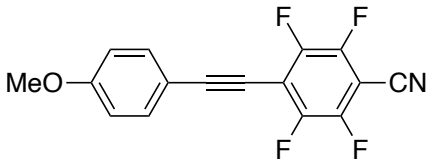

Aromatic nucleophilic substitution was carried out using pentafluorobenzonitrile (0.850 g, 4.40 mmol), 4-ethynylanisole (0.53 g, 4.0 mmol), *n*-BuLi (1.6 M in hexane) (2.5 mL, 4.00 mmol) in THF (60 mL), according to the general procedure. Purification by column chromatography (hexane : EtOAc = 20 : 1) afforded compound **2c** (0.49 g, 1.6 mmol, 40% yield, white solid). Single crystal was obtained by recrystallization from CH_2Cl_2/MeOH. m.p. = 140.2–142.2 ºC. ^{1}H NMR ($CDCl_3$): δ 3.86 (s, 3H), 6.91–6.94 (m, 2H), 7.53–7.56 (m, 2H); ^{13}C NMR ($CDCl_3$): δ 55.54, 73.09 (t, J = 4.5 Hz), 92.88 (tm, J = 17.5 Hz), 107.62 (quin, J = 3.75 Hz), 111.72 (tt, J = 18.0, 3.0 Hz), 112.73, 114.49, 134.09, 145.47 (ddt, J = 69.5, 15.0, 4.0 Hz), 148.02 (ddt, J = 78.0, 15.0, 4.5 Hz), 161.58 (one *sp*-hybridized carbon was overlapped with another sp^2-carbon); ^{19}F NMR ($CDCl_3$): δ –133.66 (ddd J = 5.0, 4.5, 1.0 Hz, 2F), –134.61 (ddd, J = 5.0, 4.5, 2.0, 2F); IR (KBr): ν 3016, 2984, 2941, 2844, 2359, 2216, 1646, 1603, 1487, 1252, 981, 836 cm^{-1}; HRMS (FAB+) *m/z* $[M]^+$ calcd for $C_{16}H_7F_4NO$: 305.0464; found: 305.0467.

NMR spectra

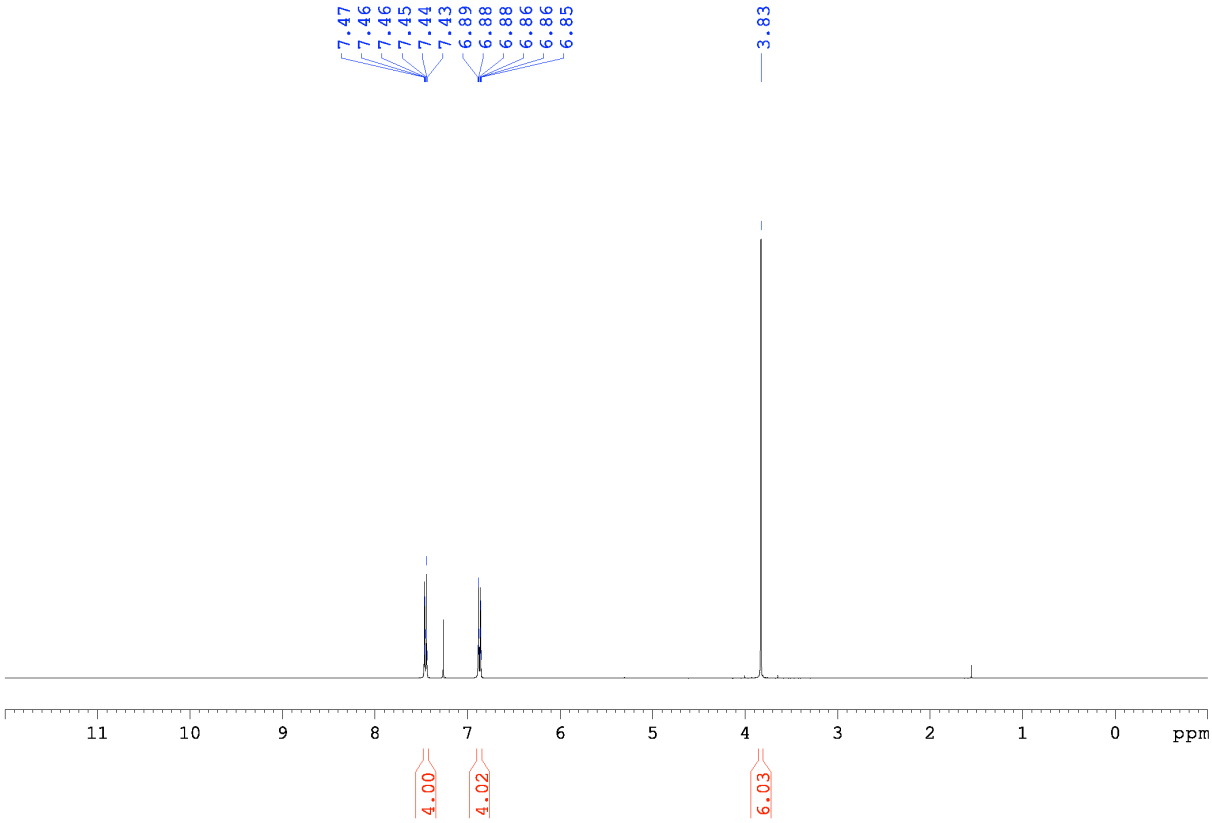

Figure S1. ^{1}H NMR spectrum of **1a**

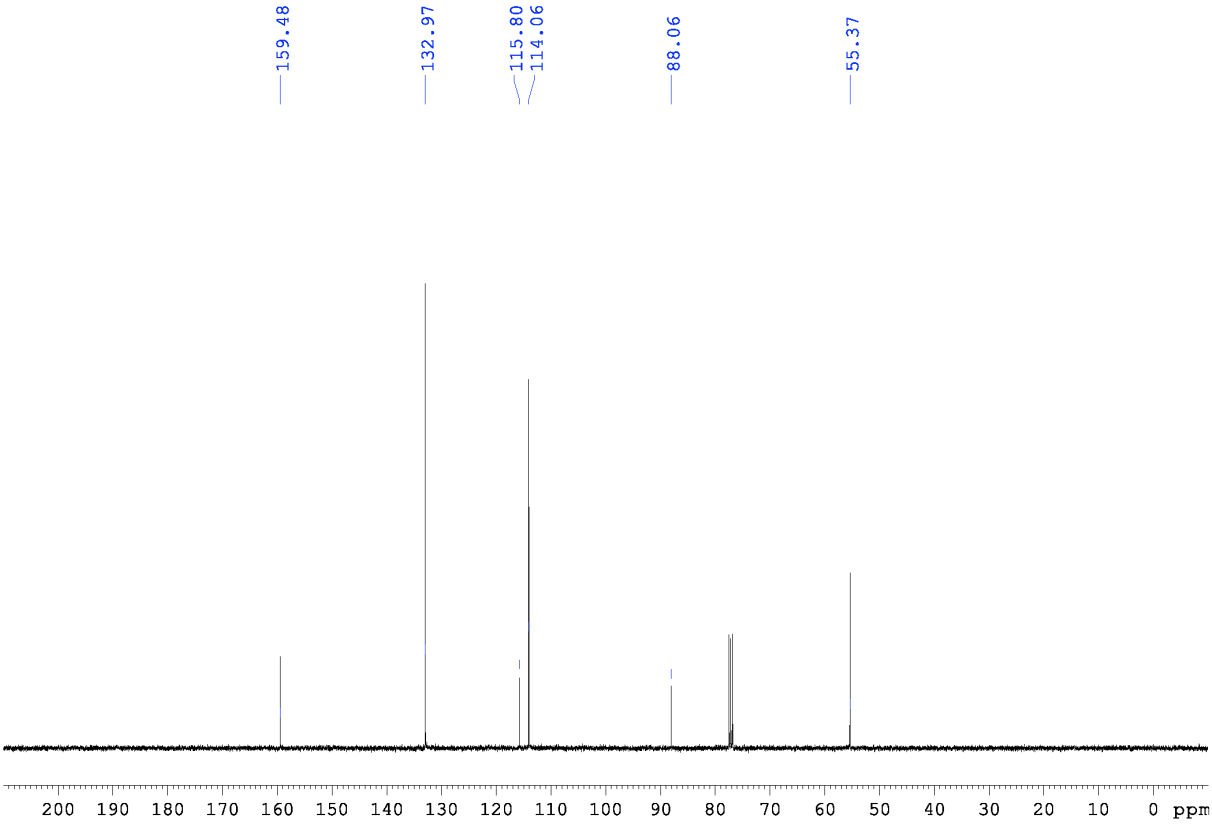

Figure S2. ^{13}C NMR spectrum of **1a**

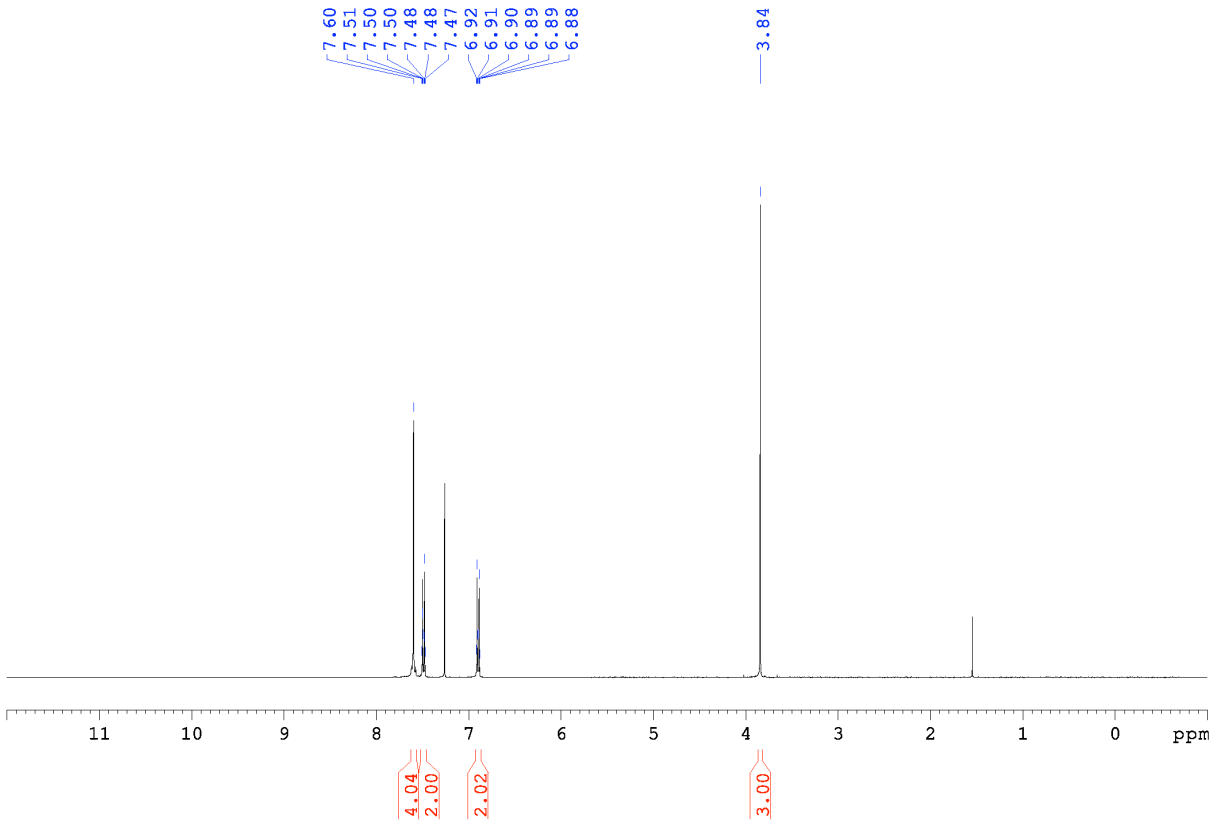

Figure S3. ^{1}H NMR spectrum of **1b**

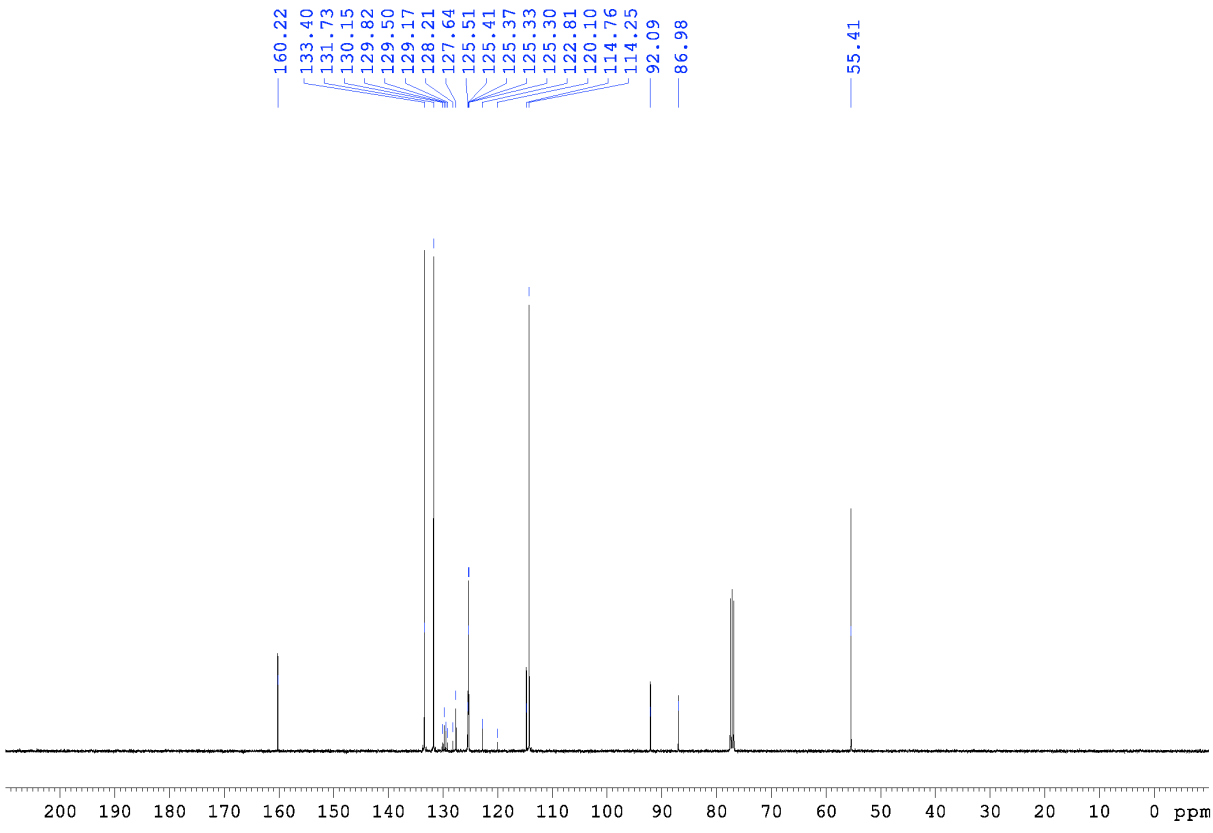

Figure S4. ^{13}C NMR spectrum of **1b**

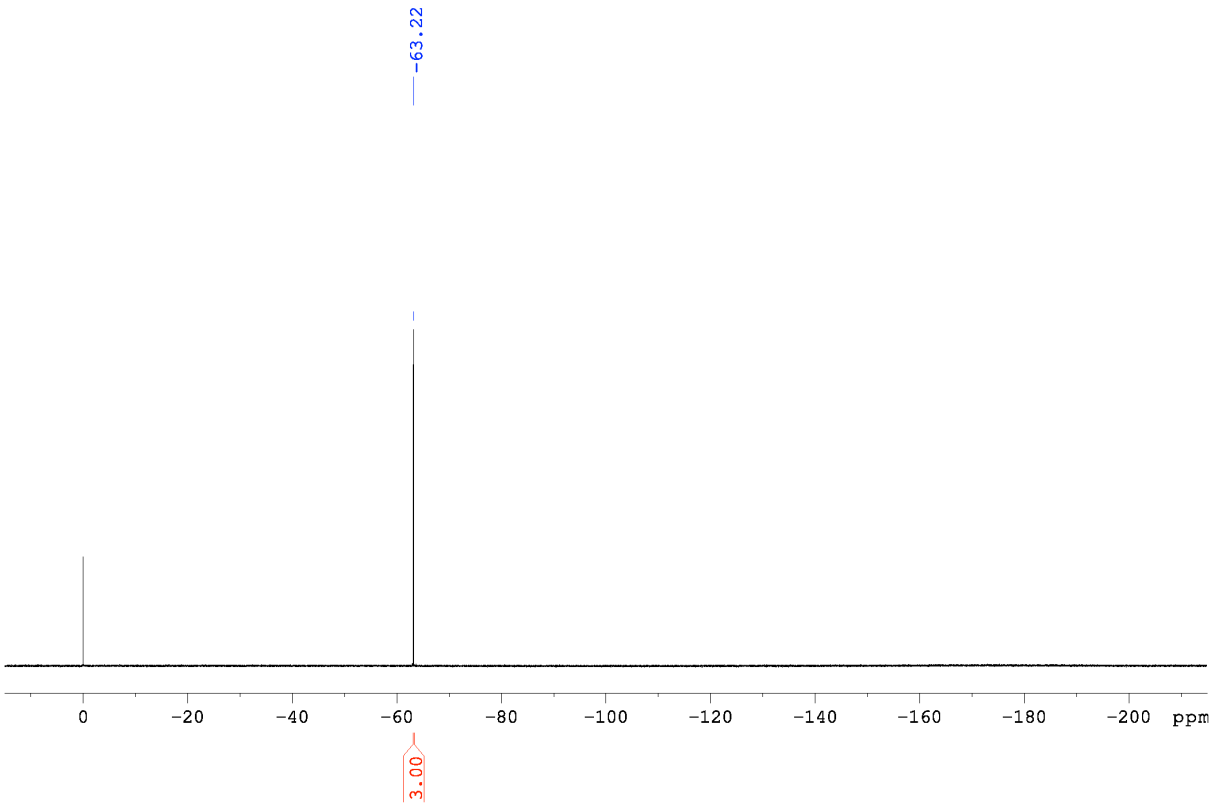

Figure S5. ^{19}F NMR spectrum of **1b**

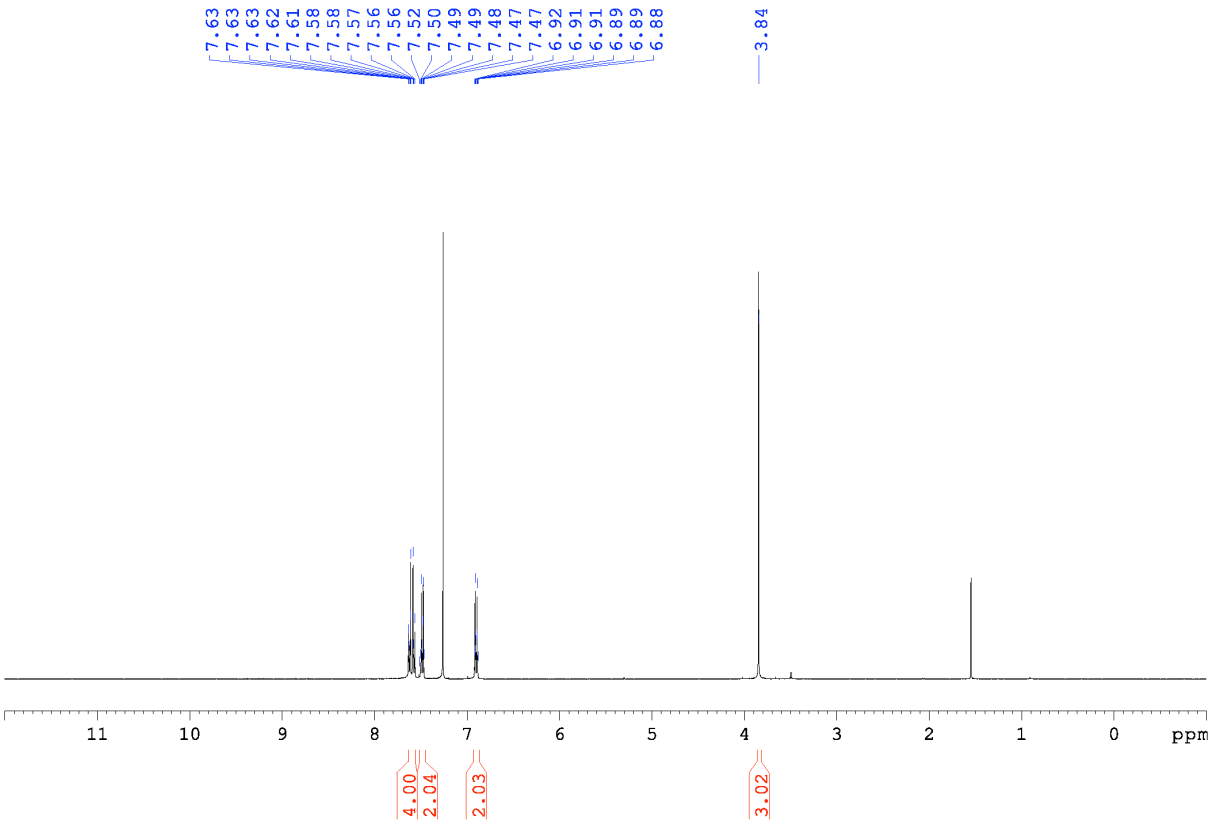

Figure S6. ^{1}H NMR spectrum of **1c**

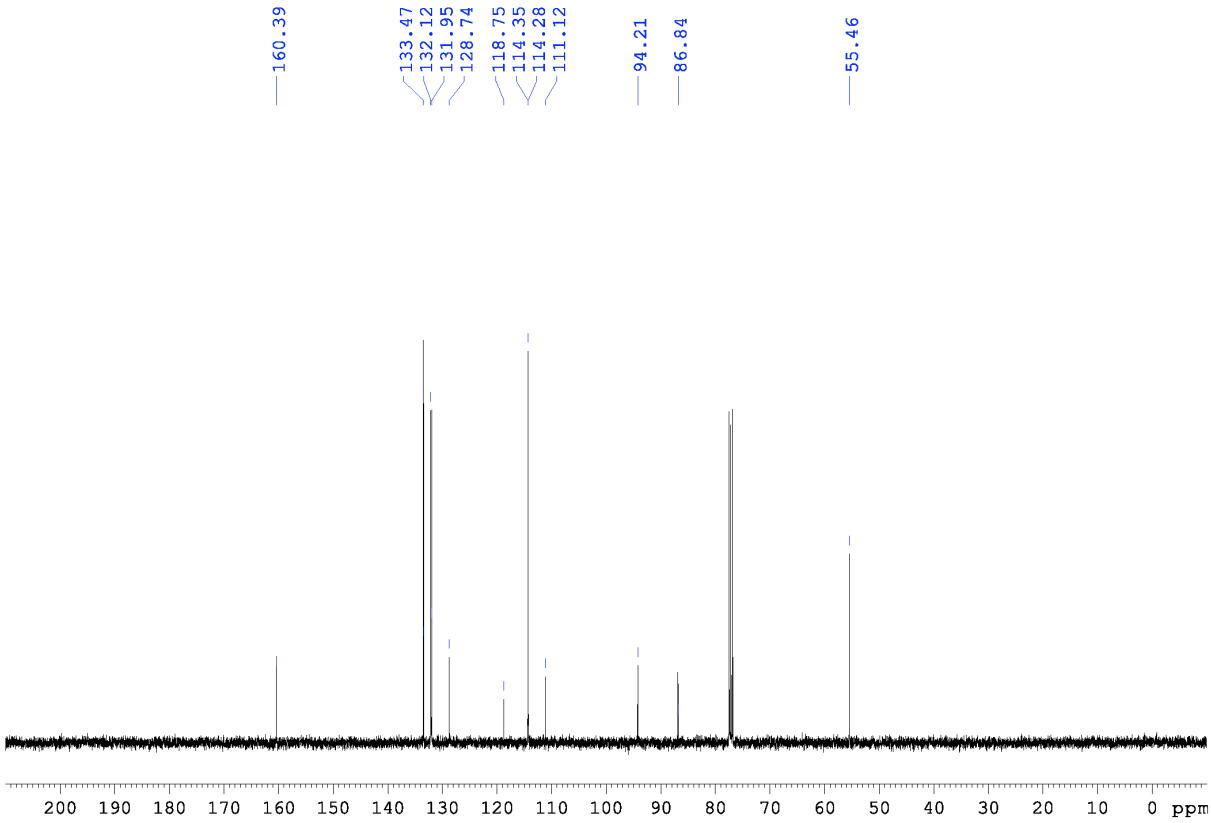

Figure S7. ^{13}C NMR spectrum of **1c**

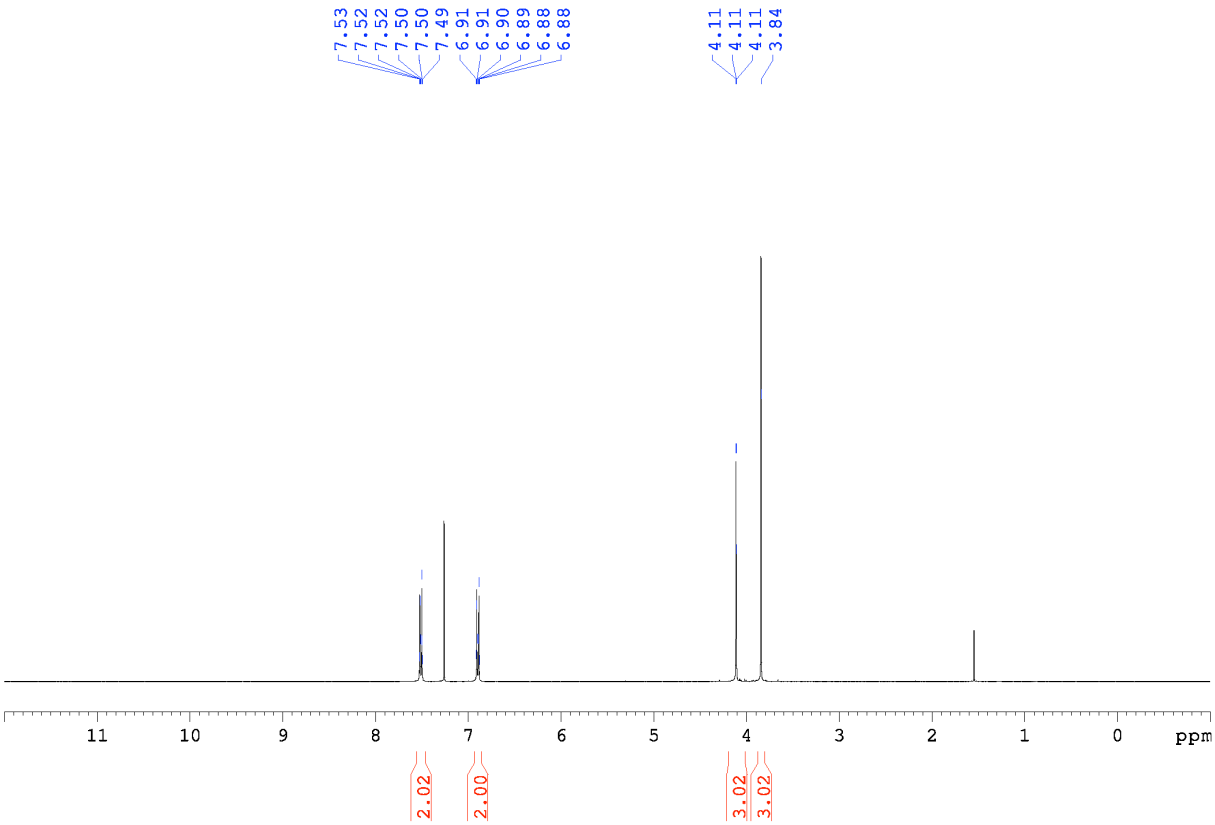

Figure S8. ^{1}H NMR spectrum of **2a**

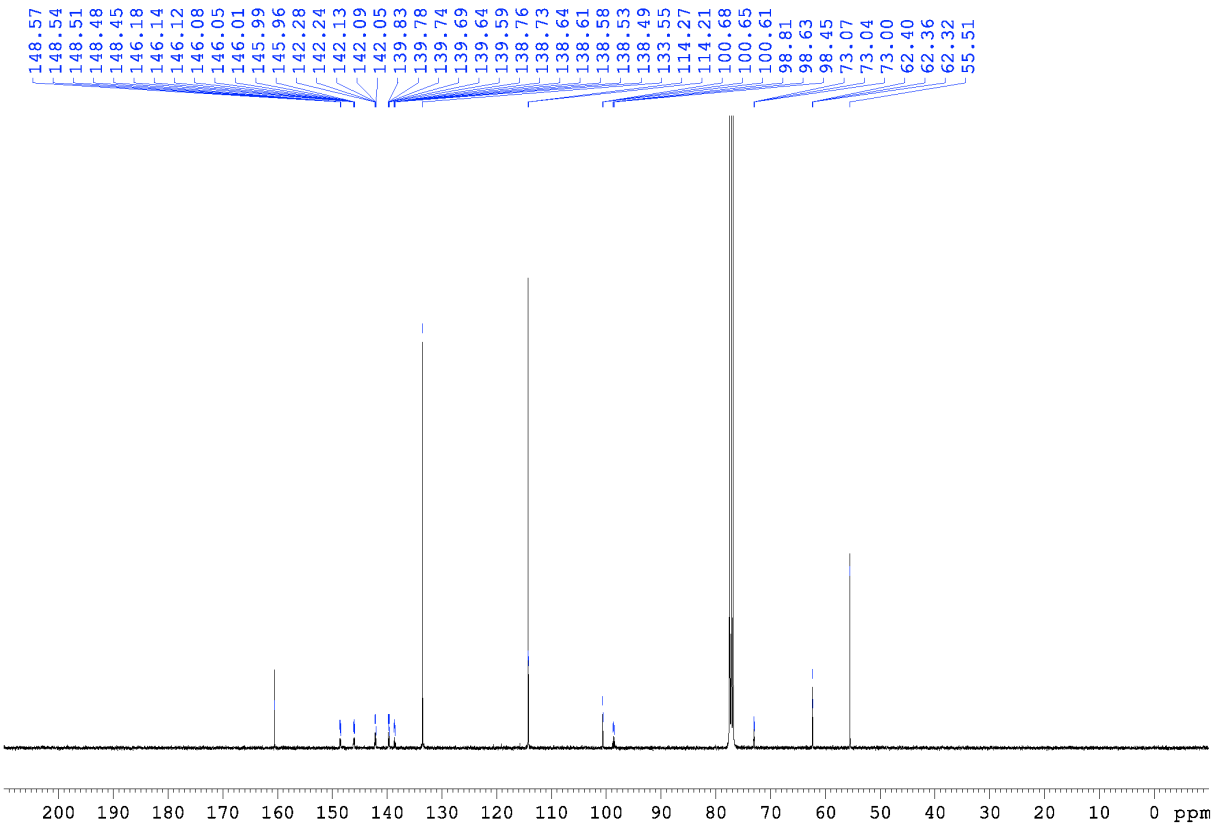

Figure S9. ^{13}C NMR spectrum of **2a**

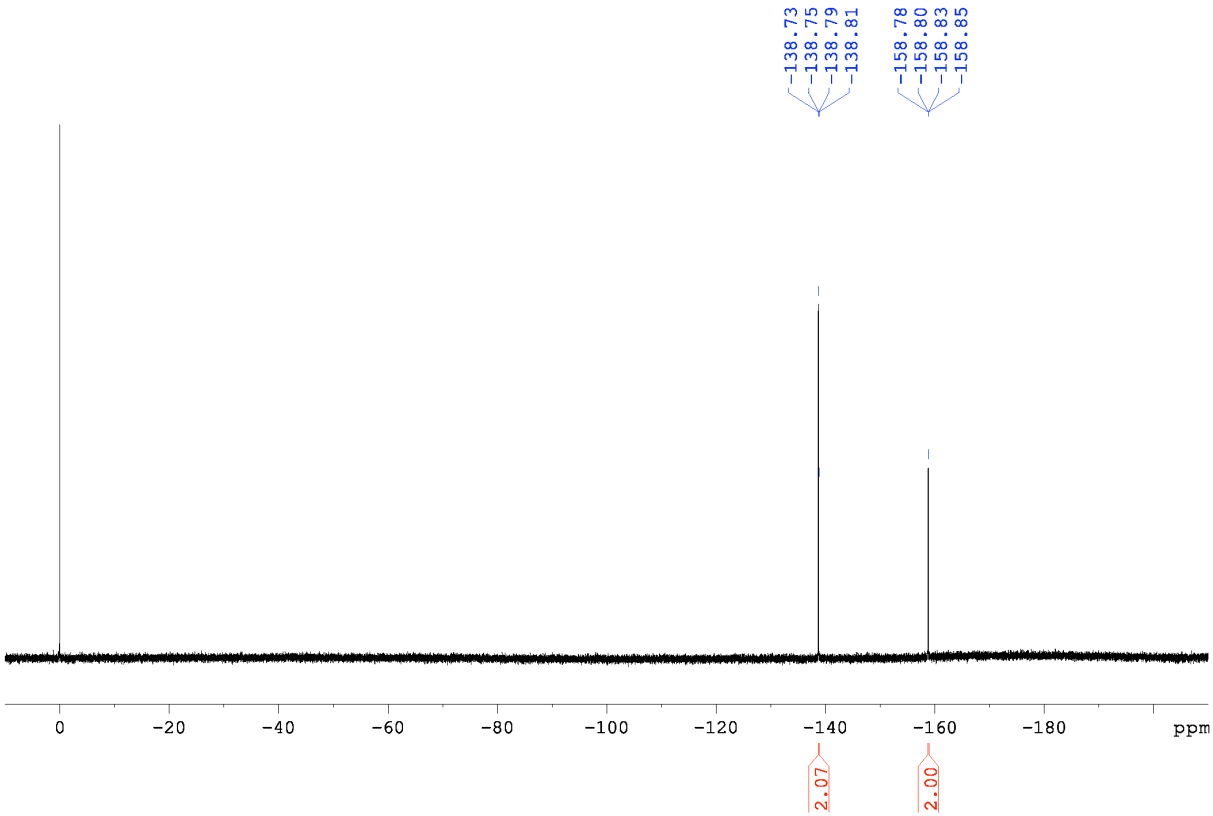

Figure S10. ^{19}F NMR spectrum of **2a**

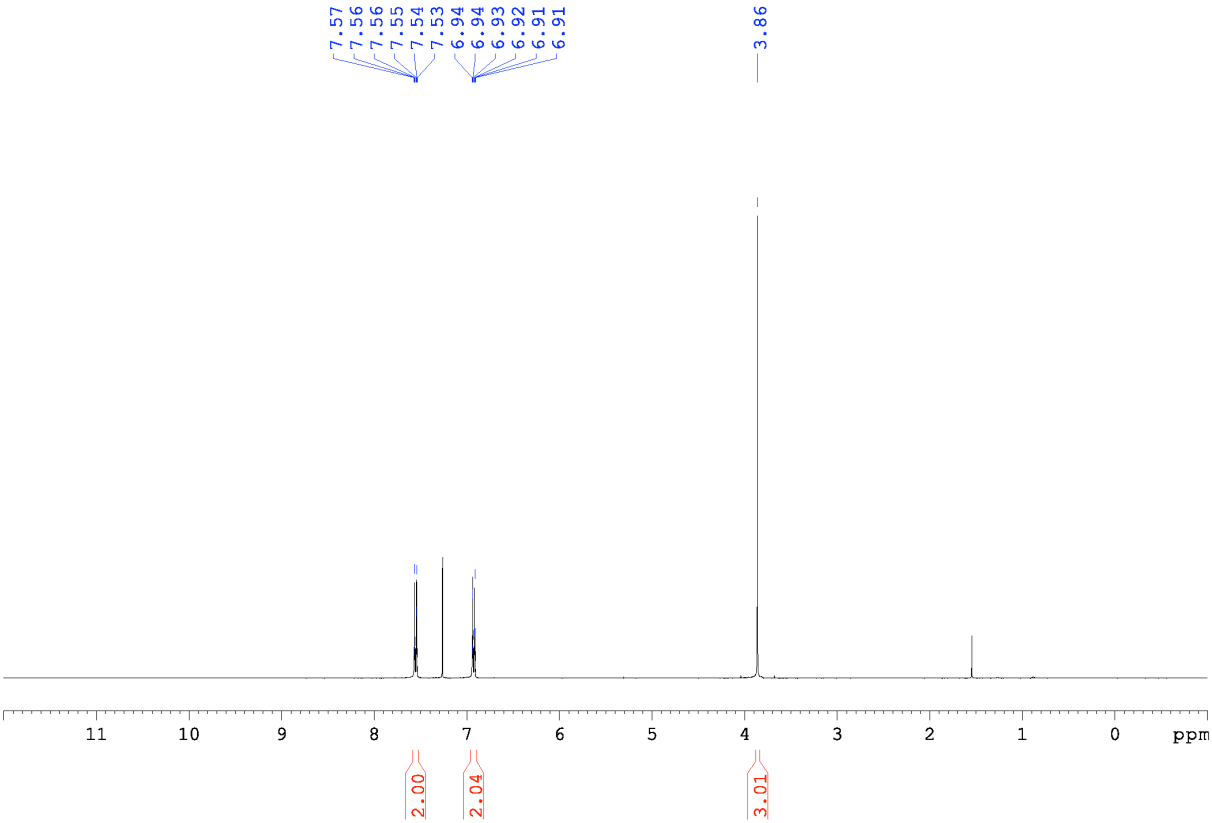

Figure S11. ^{1}H NMR spectrum of **2b**

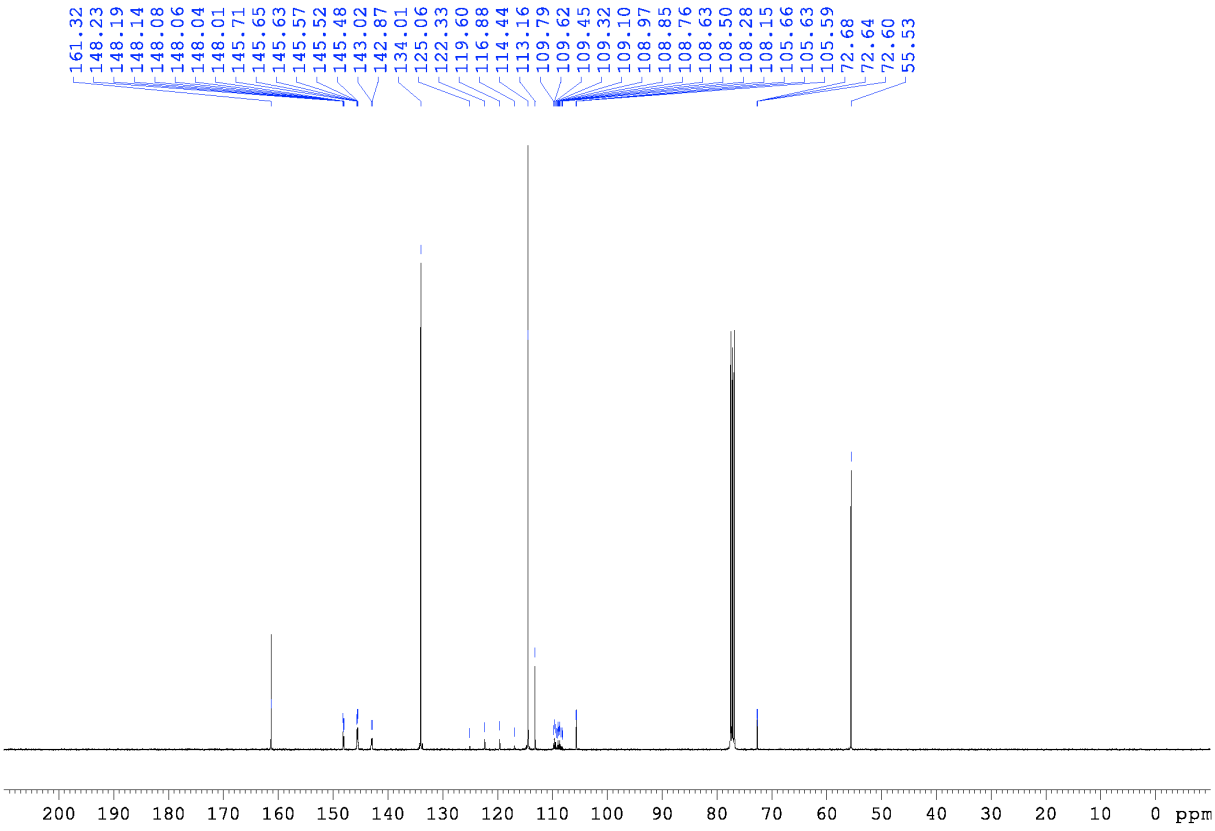

Figure S12. ^{13}C NMR spectrum of **2b**

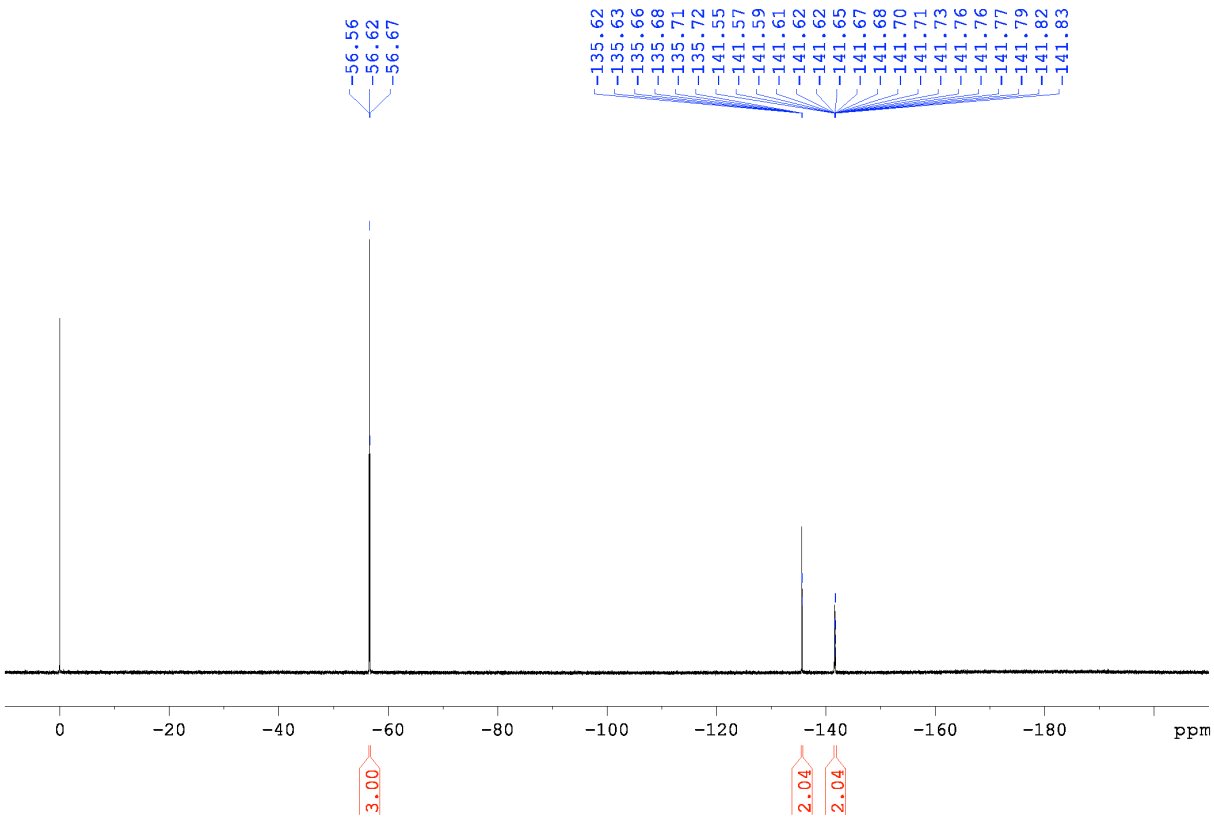

Figure S13. ^{19}F NMR spectrum of **2b**

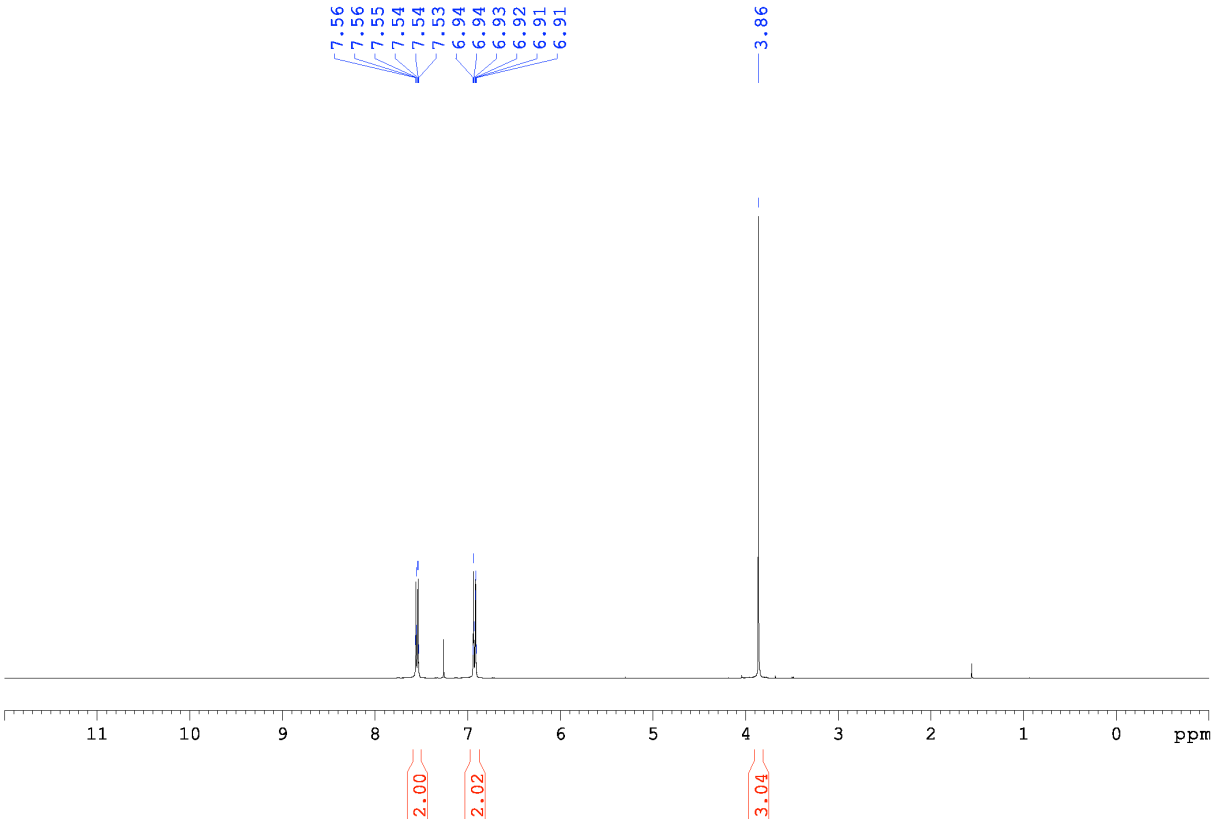

Figure S14. ^{1}H NMR spectrum of **2c**

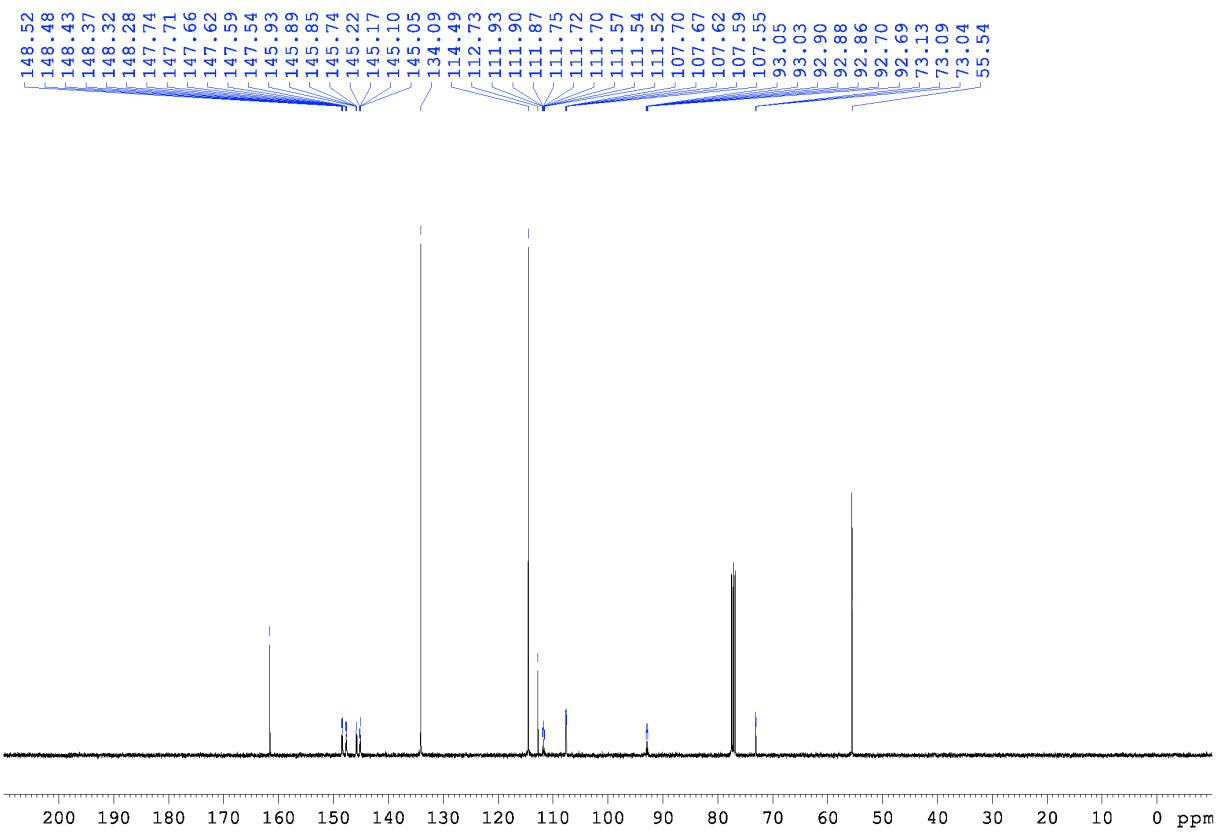

Figure S15. ^{13}C NMR spectrum of **2c**

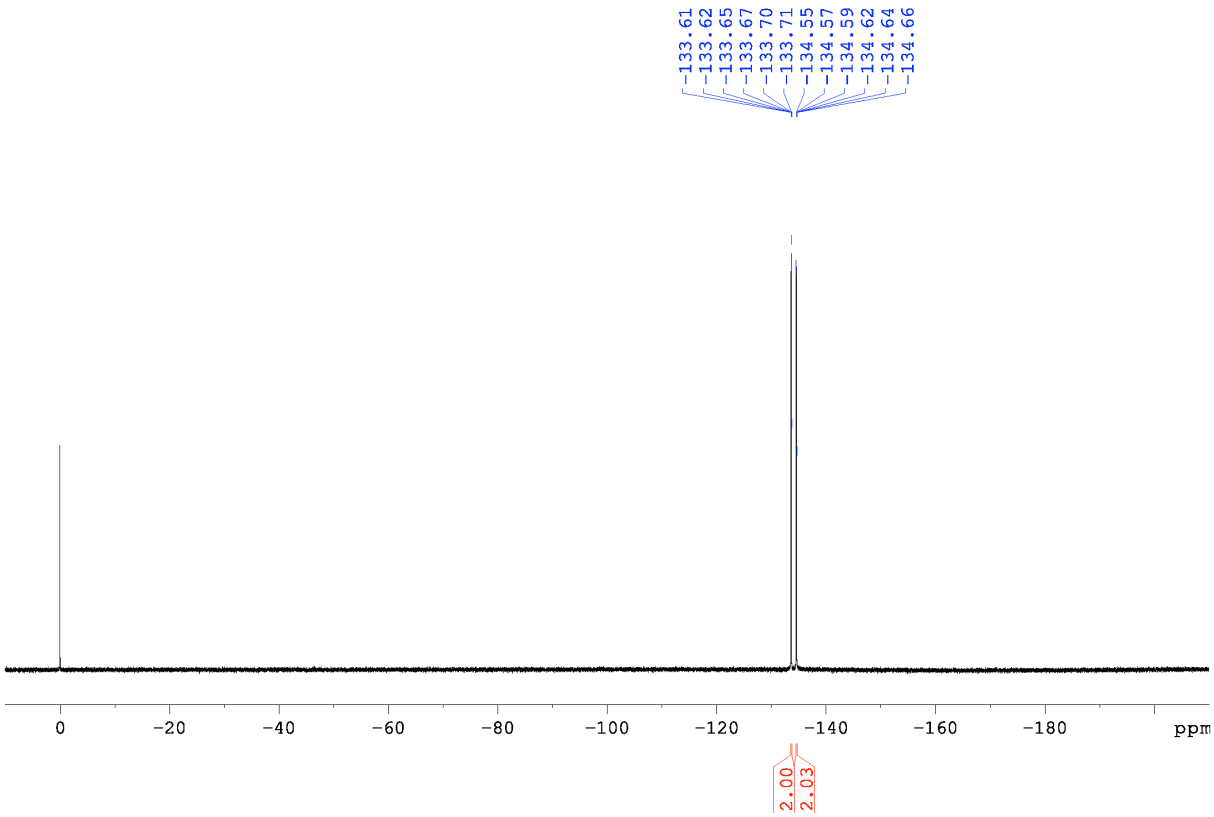

Figure S16. ^{19}F NMR spectrum of **2c**

2. Figure and Table

Supplementary photophysical data in solution:

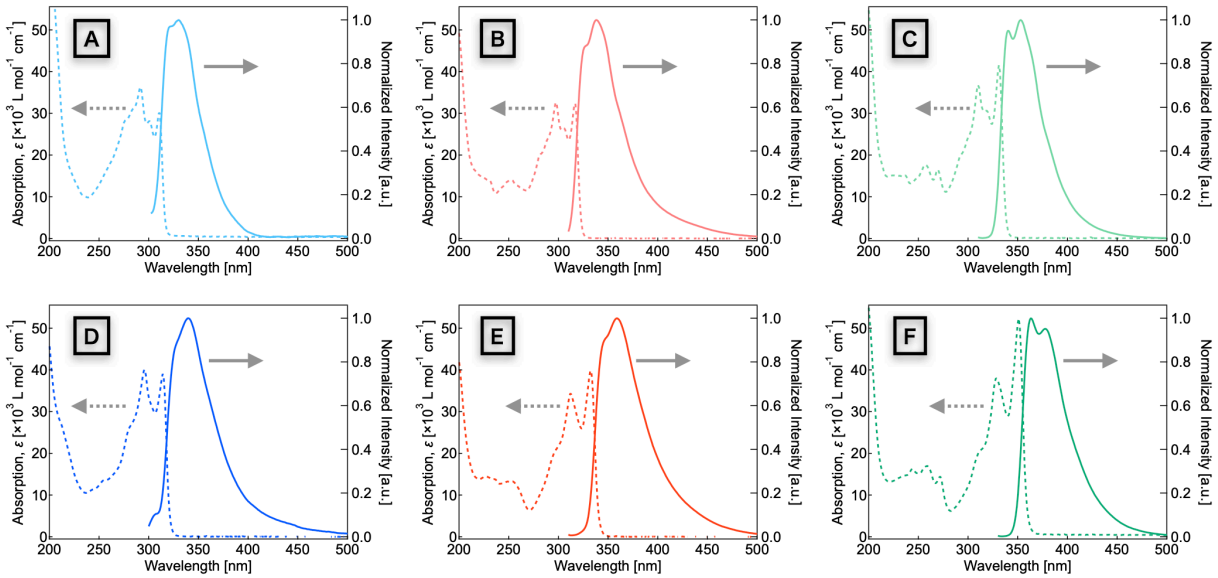

Figure S17. Absorption and PL spectra of [A] **1a**, [B] **1b**, [C] **1c**, [D] **2a**, [E] **2b**, and [F] **2c** in hexane

Table S1 Photophysical properties in 10^{-5} mol L^{-1} hexane.

	λ_{abs}/nm (ε /10^3 L mol^{-1} cm^{-1})	λ_{max}/nm	Φ_{em}
1a	292 (36), 311 (30)	313sh, 330	0.02
1b	298 (33), 317 (32)	324sh, 338	0.02
1c	310 (37), 331 (42)	340sh, 353	0.17
2a	296 (40), 314 (39)	322sh, 340	0.02
2b	312 (34), 332 (40)	343sh, 359	0.04
2c	328 (38), 351 (52)	363, 378sh	0.18

Table S2 HOMO, LUMO, and ΔE.[a]

	HOMO/eV	LUMO/eV	ΔE/eV
1a	–6.6382	–0.3037	–6.3345
1b	–7.2091	–1.0221	–6.1871
1c	–7.2698	–1.3540	–5.9158
2a	–7.1229	–0.8925	–6.2303
2b	–7.5620	–1.6232	–5.9389
2c	–7.6260	–1.9927	–5.6333

[a] Calculated using Gaussian 16 with DFT method with CPCM for heptane.

Table S3 Photophysical properties of **1c** in 10^{-4} mol L^{-1} THF/water mixture.

Water ratio [%]	PL intensity [a.u.]	λ_{max}/nm	Φ_{em}
0	618	386	0.15
10	535	393	0.16
20	505	410	0.16
30	503	411	0.17
40	486	415	0.17
50	467	415	0.17
60	435	420	0.17
70	388	423	0.16
80	270	433	0.13
85	225	393, 410sh	0.12
90	266	391, 406sh	0.13

Table S4 Photophysical properties of **2c** in 10^{-4} mol L^{-1} THF/water mixture.

Water ratio [%]	PL intensity [a.u.]	λ_{max}/nm	Φ_{em}
0	304	457	0.14
10	184	484	0.12
20	137	495	0.09
30	111	512	0.08
40	92	511	0.07
50	75	512	0.06
60	57	523	0.04
70	56	501	0.04
80	309	474	0.17
85	470	474	0.28
90	596	475	0.41

Photophysical properties in different solvents:

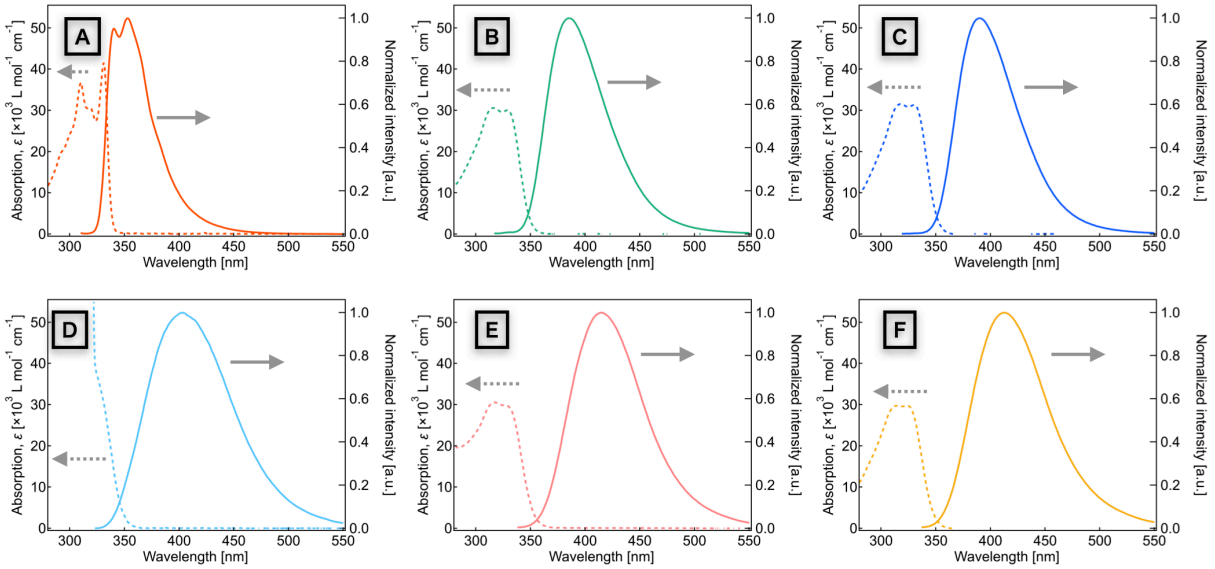

Figure S18. UV-vis and PL spectra of **1c** in [A] hexane ($E_T(30)$ = 31.0), [B] THF ($E_T(30)$ = 37.4), [C] CH_2Cl_2 ($E_T(30)$ = 40.7), [D] Acetone ($E_T(30)$ = 42.2), [E] DMF ($E_T(30)$ = 43.2), [F] Acetonitrile ($E_T(30)$ = 45.6).

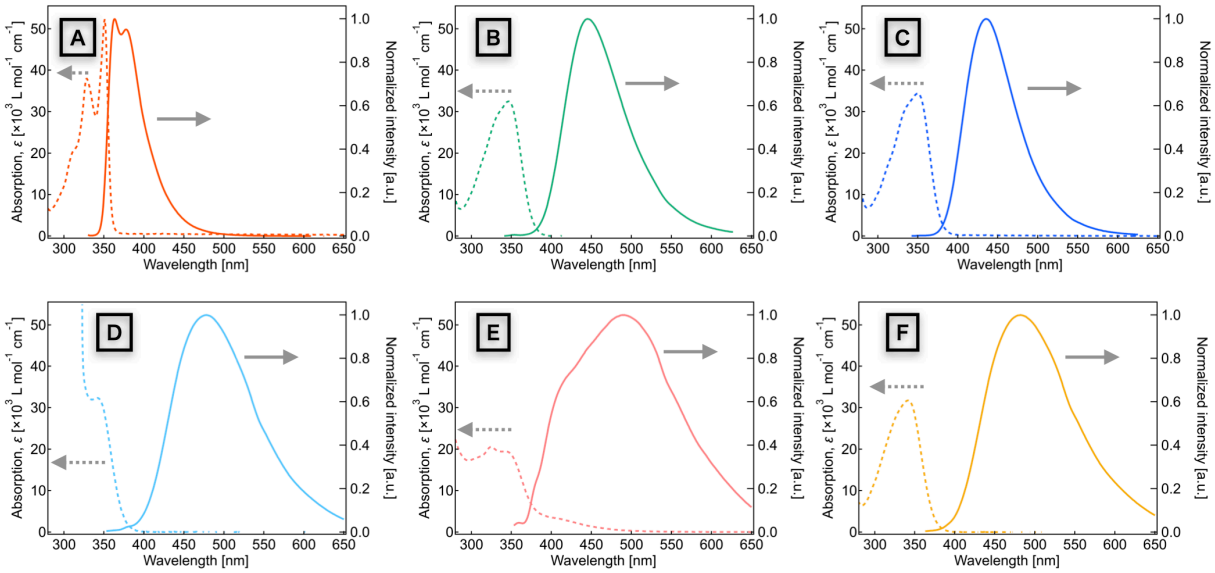

Figure S19. UV-vis and PL spectra of **2c** in [A] hexane ($E_T(30)$ = 31.0), [B] THF ($E_T(30)$ = 37.4), [C] CH_2Cl_2 ($E_T(30)$ = 40.7), [D] Acetone ($E_T(30)$ = 42.2), [E] DMF ($E_T(30)$ = 43.2), [F] Acetonitrile ($E_T(30)$ = 45.6).

Lippert-Mataga Plot:[5]

$$\upsilon_A - \upsilon_F = \Delta\upsilon = \frac{2}{hca_0^3}\left(\frac{\epsilon-1}{2\epsilon+1} - \frac{n^2-1}{2n^2+1}\right)(\mu_e - \mu_g)^2 = \frac{2\Delta f}{hca_0^3}\Delta\mu^2$$

Where h is the Plank's constant, c is the velocity of light, and a_0 is Onsager cavity radius. The solvent parameters ε and n are solvent dielectric constant and refraction index, respectively. The Onsager radius (a_0 = 5.12 Å for **1c** and 5.11 Å for **2c**) was calculated from DFT optimization.

Table S5. Photophysical properties of **1c** in different solvents.

	ε	n	Δf	ν_A/cm^{-1}	ν_F/cm^{-1}	$\Delta\nu$/cm^{-1}
Hexane	1.88	1.37	0.0004	30211	28328	1883
THF	7.58	1.41	0.209	30395	25974	4421
CH_2Cl_2	8.93	1.42	0.219	30395	25641	4754
Acetone	20.6	1.36	0.284	30769	24814	5945
DMF	36.7	1.43	0.275	30864	24096	6768
MeCN	35.9	1.34	0.306	30211	24213	5998

Table S6. Photophysical properties of **2c** in different solvents.

	ε	n	Δf	ν_A/cm^{-1}	ν_F/cm^{-1}	$\Delta\nu$/cm^{-1}
Hexane	1.88	1.37	0.0004	28490	27548	942
THF	7.58	1.41	0.209	28901	22471	6430
CH_2Cl_2	8.93	1.42	0.219	28571	22988	5583
Acetone	20.6	1.36	0.284	28735	20920	7815
DMF	36.7	1.43	0.275	28571	20450	8121
MeCN	35.9	1.34	0.306	29325	20747	8578

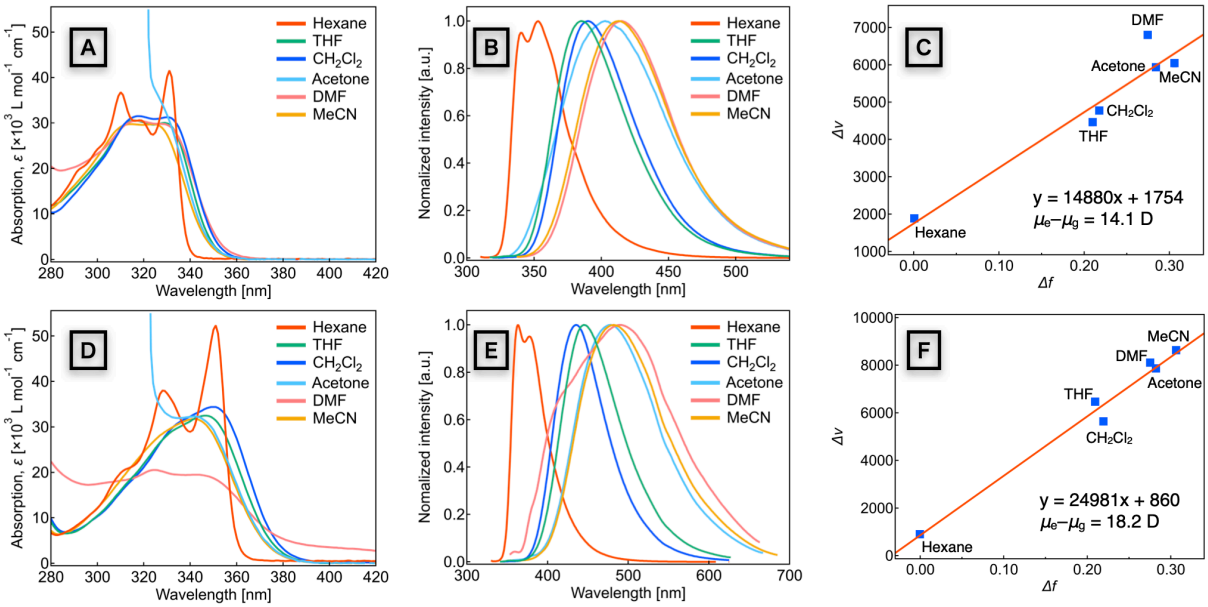

Figure S20. [A] UV-vis spectra of **1c**, [b] PL spectra of **1c**, [C] Lippert-Mataga Plot for **1c**, [D] UV-vis spectra of **2c**, [E] PL spectra of **2c**, [F] Lippert-Mataga Plot for **2c**.

Supplementary photophysical data in crystal:

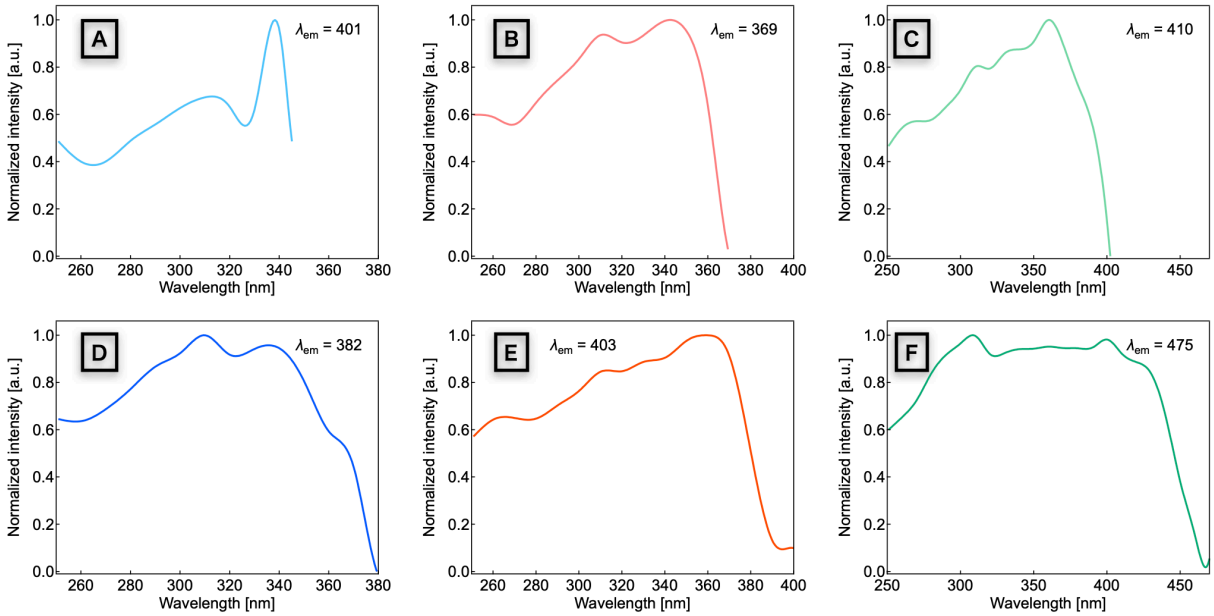

Figure S21. Excitation spectra of [A] **1a**, [B] **1b**, [C] **1c**, [D] **2a**, [E] **2b**, and [F] **2c** in crystal

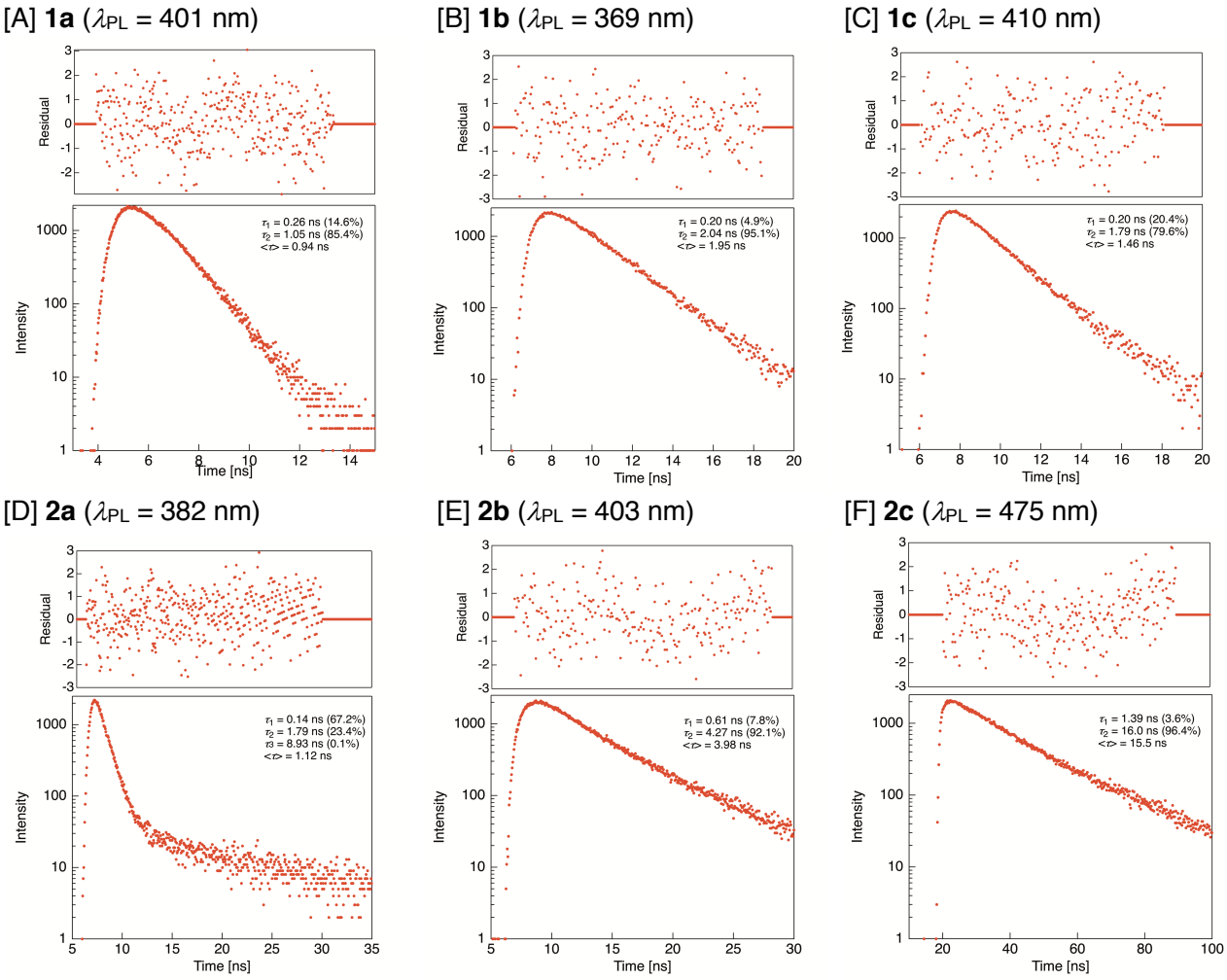

Figure S22. Photoluminescence decay profiles for **1a–c** and **2a–c** in crystal obtained using Quantaurus-Tau fluorescence lifetime spectrometer.

Table S7 Photophysical properties in crystal.[a]

	λ_{ex}/nm	λ_{max}/nm	Φ_{em} / $<\tau>^{b}$ [ns]
1a	310	388sh, 401, 421sh	0.03 / 0.94
1b	310	369	0.40 / 1.95
1c	310	385sh, 410, 438sh	0.17 / 1.46
2a	310	366sh, 382	0.18 / 1.12
2b	310	403	0.73 / 3.98
2c	310	475	0.93 / 15.5

[a] Observed using Quantaurus-QY absolute quantum yield spectrometer. [b] Average lifetime obtained by using Quantaurus-Tau fluorescence lifetime spectrometer.

Supplementary crystallographic data

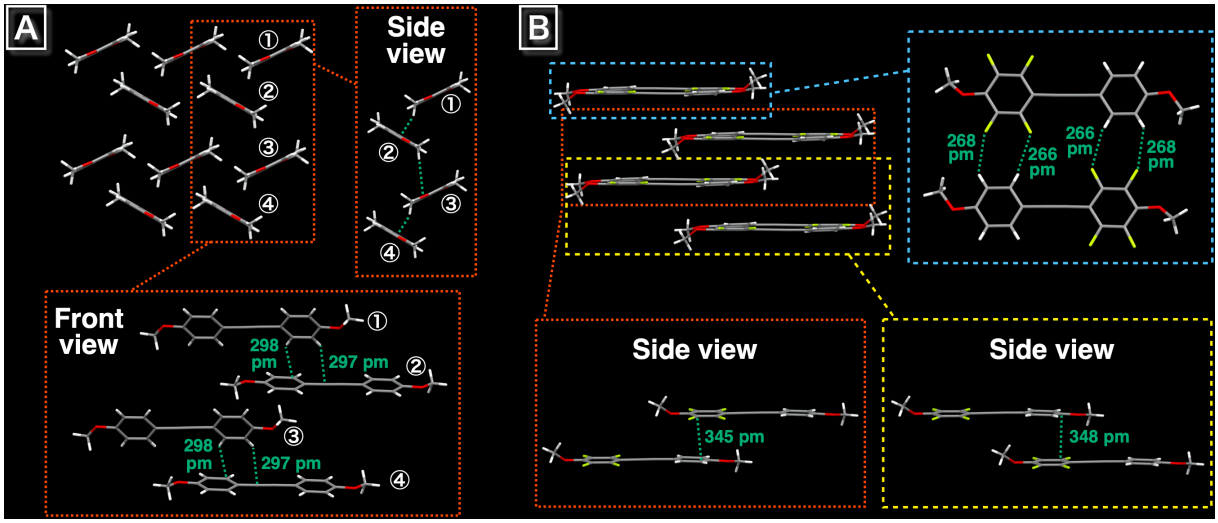

Figure S23. Packing structure of [A] **1a**, [B] **2a**

Table S8. Crystallographic data of **1a–c**

	1a	**1b**	**1c**
CCDC #	1982046	1982047	1982048
Empirical Formula	$C_{16}H_{14}O_2$	$C_{16}H_{11}F_3O$	$C_{16}H_{11}NO$
Formula weight	238.27	276.25	233.26
Temperature [K]	293	293	293
Crystal Color / Habit	Colorless / Block	Colorless / Block	Colorless / Block
Crystal Size [mm]	0.34 × 0.47 × 0.61	0.37 × 0.46 × 0.50	0.14 × 0.58 × 0.67
Crystal System	monoclinic	orthorhombic	monoclinic
Space Group	$P2_1/c$	$Pca2_1$	$P2_1/c$
a [Å]	8.5051(5)	6.2167(3)	6.0792(3)
b [Å]	5.7663(3)	7.5783(4)	7.7395(3)
c [Å]	13.3375(7)	28.6871(14)	28.2605(15)
α [°]	90	90	90
β [°]	90.705(5)	90	106.747(5)
γ [°]	90	90	90
V [Å^3]	654.06(6)	1351.51(12)	1273.26(11)
Z	2	4	4
R [$F^2 > 2\sigma(F^2)$] [a]	0.0432	0.0574	0.0466
$wR2$ (F^2) [b]	0.1229	0.1998	0.1533

[a] $R = \Sigma||F_o| - |F_c|| / \Sigma|F_o|$. [b] $wR = \{[\Sigma w(|F_o| - |F_c|)]/\Sigma w|F_o|\}^{1/2}$.

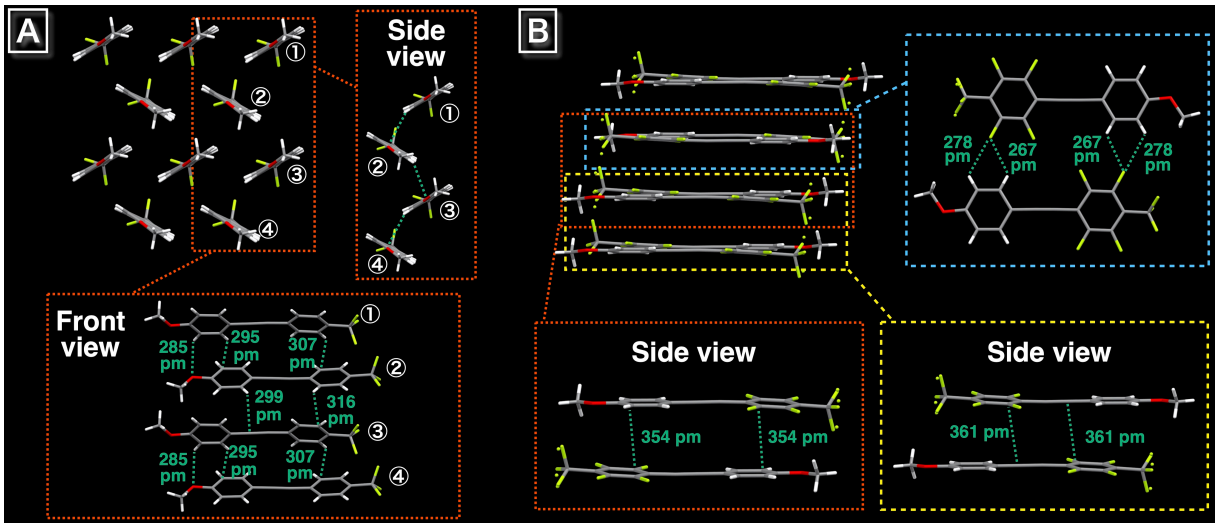

Figure S24. Packing structure of [A] **1b**, [B] **2b**

Table S9. Crystallographic data of **2a–c**

	2a	**2b**	**2c**
CCDC #	1982049	1982050	1982051
Empirical Formula	$C_{16}H_{10}F_4O_2$	$C_{16}H_7F_7O$	$C_{16}H_7F_4NO$
Formula weight	310.24	348.22	305.23
Temperature [K]	293	293	298
Crystal Color / Habit	Colorless / Block	Colorless / Plate	Colorless / Block
Crystal Size [mm]	0.21 × 0.28 × 0.35	0.11 × 0.35 × 0.58	0.14 × 0.30 × 0.34
Crystal System	triclinic	triclinic	triclinic
Space Group	*P*-1	*P*-1	*P*-1
a [Å]	7.3516(4)	5.6304(5)	6.2399(3)
b [Å]	8.5060(5)	8.4095(9)	7.7358(3)
c [Å]	12.5385(7)	15.7707(14)	28.6607(8)
α [°]	100.778(5)	95.118(8)	95.911(2)
β [°]	96.710(4)	96.805(7)	90.746(3)
γ [°]	113.627(5)	92.702(8)	98.579(3)
V [Å^3]	689.46(7)	737.25(12)	1360.15(9)
Z	2	2	4
$R\,[F^2 > 2\sigma(F^2)]$ [a]	0.0434	0.0469	0.0422
$wR2\,(F^2)$ [b]	0.1455	0.1675	0.1558

[a] $R = \Sigma||F_o| - |F_c|| / \Sigma|F_o|$. [b] $wR = \{[\Sigma w(|F_o| - |F_c|)]/\Sigma w|F_o|\}^{1/2}$.

3. Geometry optimization

3-1. Geometry optimization for 1a

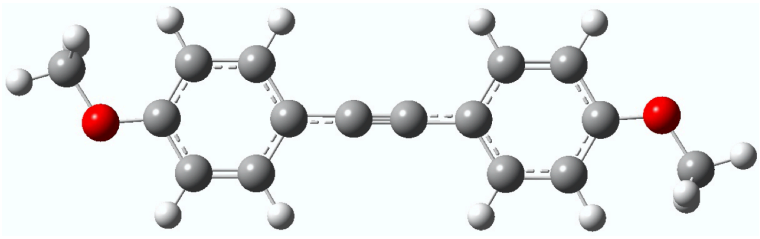

No.	Atom No.	Type	Coordinates (Angstroms) x	y	z
1	6	0	-4.064372	1.446411	-0.000009
2	6	0	-2.683039	1.365923	-0.000007
3	6	0	-2.035537	0.115783	0.000001
4	6	0	-2.820961	-1.042527	0.000008
5	6	0	-4.212960	-0.971314	0.000006
6	6	0	-4.839141	0.278178	-0.000003
7	1	0	-4.571584	2.406074	-0.000016
8	1	0	-2.086939	2.273331	-0.000012
9	1	0	-2.335593	-2.013782	0.000015
10	1	0	-4.789525	-1.888937	0.000012
11	6	0	-0.606047	0.033221	0.000003
12	6	0	0.606047	-0.033224	0.000003
13	6	0	2.035537	-0.115785	0.000001
14	6	0	2.820960	1.042526	0.000008
15	6	0	2.683040	-1.365924	-0.000007
16	6	0	4.212959	0.971315	0.000007
17	1	0	2.335591	2.013781	0.000015
18	6	0	4.064374	-1.446411	-0.000008
19	1	0	2.086941	-2.273333	-0.000011
20	6	0	4.839141	-0.278177	-0.000002
21	1	0	4.789523	1.888938	0.000012
22	1	0	4.571586	-2.406073	-0.000015
23	8	0	6.184441	-0.460295	-0.000005
24	6	0	7.007868	0.691455	0.000004
25	1	0	6.834449	1.298545	0.895832
26	1	0	8.034042	0.325914	0.000003
27	1	0	6.834450	1.298558	-0.895814
28	8	0	-6.184441	0.460298	-0.000005
29	6	0	-7.007868	-0.691452	0.000003
30	1	0	-8.034042	-0.325910	0.000000
31	1	0	-6.834451	-1.298555	-0.895816
32	1	0	-6.834451	-1.298542	0.895830

Dipole moment (field-independent basis, Debye):

X = 0.0000, Y = 0.0000, Z = 0.0000, Tot = 0.0000

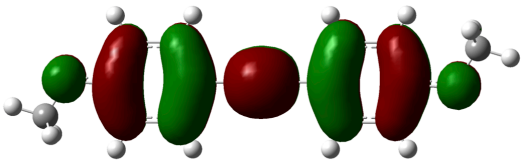

HOMO 63

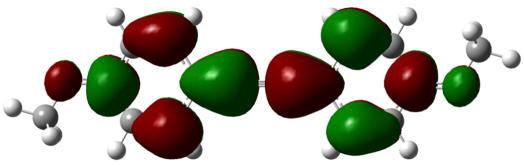

LUMO 64

Excited State 1: Singlet-A 4.2900 eV 289.01 nm *f*=1.4463 <S**2>=0.000

63 -> 64 0.69100

3-2. Geometry optimization for 1b

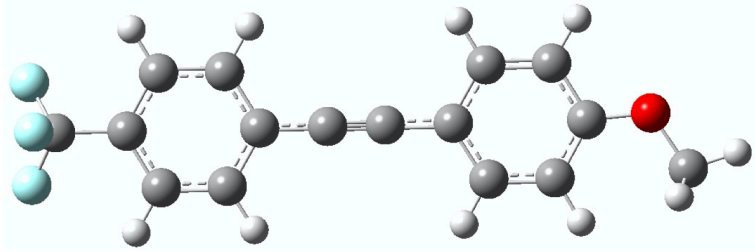

No.	Atom No.	Type	Coordinates (Angstroms) x	y	z
1	6	0	4.871805	1.405111	0.010012
2	6	0	3.489334	1.367589	0.000838
3	6	0	2.805693	0.136812	-0.009047
4	6	0	3.553145	-1.046431	-0.009705
5	6	0	4.945848	-1.018212	-0.000598
6	6	0	5.609690	0.212436	0.009547
7	1	0	5.409104	2.348074	0.017984
8	1	0	2.920976	2.292550	0.001490
9	1	0	3.037392	-2.001805	-0.017354
10	1	0	5.494432	-1.952710	-0.001323
11	6	0	1.375453	0.097526	-0.017237
12	6	0	0.162371	0.066357	-0.022937
13	6	0	-1.268480	0.031209	-0.027135
14	6	0	-2.006630	1.226194	-0.030840
15	6	0	-1.948515	-1.197334	-0.029379
16	6	0	-3.394992	1.192204	-0.034798
17	1	0	-1.482573	2.176288	-0.032805
18	6	0	-3.337416	-1.230113	-0.033052
19	1	0	-1.379614	-2.121286	-0.030192
20	6	0	-4.056693	-0.035689	-0.036791
21	1	0	-3.962694	2.117420	-0.041374
22	1	0	-3.859722	-2.181489	-0.038200
23	8	0	6.957589	0.352869	0.019510
24	6	0	7.747990	-0.822900	0.021220
25	1	0	7.549560	-1.427469	0.913304
26	1	0	7.564145	-1.420346	-0.878752
27	1	0	8.783856	-0.486446	0.030995
28	6	0	-5.556620	-0.067328	0.014885
29	9	0	-6.108958	0.978162	-0.626210
30	9	0	-6.016405	-0.023370	1.283231
31	9	0	-6.062134	-1.184829	-0.535881

Dipole moment (field-independent basis, Debye):

X = 5.1902, Y = -1.3977, Z = -0.0978, Tot = 5.3761

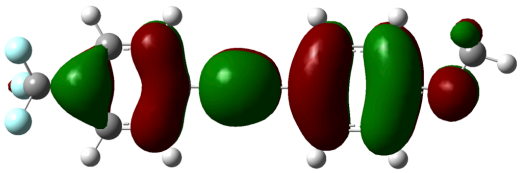

HOMO 71

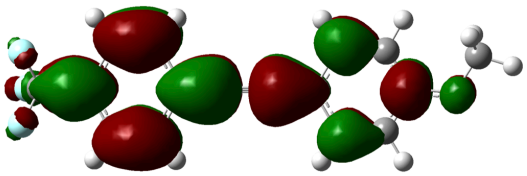

LUMO 72

Excited State 1: Singlet-A 4.2015 eV 295.10 nm *f*=1.3304 <S**2>=0.000

71 -> 72 0.68592

3-3. Geometry optimization for 1c

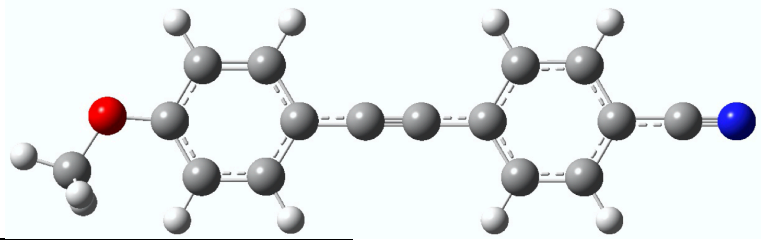

No.	Atom No.	Type	Coordinates (Angstroms) x	y	z
1	6	0	3.902080	1.409178	-0.000010
2	6	0	2.519961	1.365716	-0.000047
3	6	0	1.841938	0.131634	-0.000062
4	6	0	2.594271	-1.048692	-0.000039
5	6	0	3.986649	-1.014338	-0.000002
6	6	0	4.645104	0.219465	0.000013
7	1	0	4.435464	2.354362	0.000001
8	1	0	1.947498	2.288123	-0.000066
9	1	0	2.082565	-2.006258	-0.000051
10	1	0	4.539450	-1.946317	0.000015
11	6	0	0.412424	0.086246	-0.000107
12	6	0	-0.800767	0.050386	-0.000131
13	6	0	-2.230046	0.010389	-0.000065
14	6	0	-2.972016	1.203963	-0.000017
15	6	0	-2.905899	-1.221849	-0.000056
16	6	0	-4.358646	1.168320	0.000039
17	1	0	-2.450546	2.155389	-0.000025
18	6	0	-4.292451	-1.261681	0.000000
19	1	0	-2.333311	-2.143425	-0.000095
20	6	0	-5.021578	-0.065657	0.000048
21	1	0	-4.932572	2.089163	0.000076
22	1	0	-4.815241	-2.212506	0.000006
23	8	0	5.991827	0.365813	0.000049
24	6	0	-6.460136	-0.104902	0.000106
25	7	0	-7.617820	-0.136652	0.000152
26	6	0	6.788202	-0.806204	0.000071
27	1	0	6.599956	-1.407955	0.896198
28	1	0	6.599999	-1.407959	-0.896062
29	1	0	7.822319	-0.464393	0.000095

Dipole moment (field-independent basis, Debye):

X = 7.3350, Y = -1.3091, Z = -0.0001, Tot = 7.4509

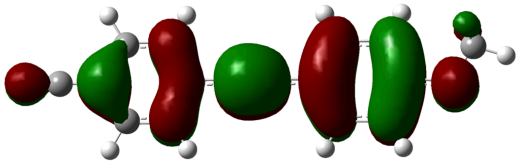

HOMO 61

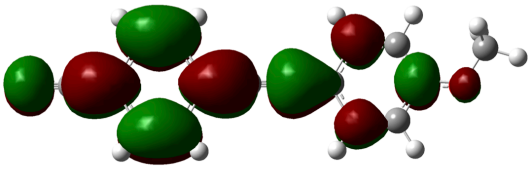

LUMO 62

Excited State 1: Singlet-A 4.0095 eV 309.23 nm *f*=1.4673 <S**2>=0.000

61 -> 62 0.68365

3-4. Geometry optimization for 2a

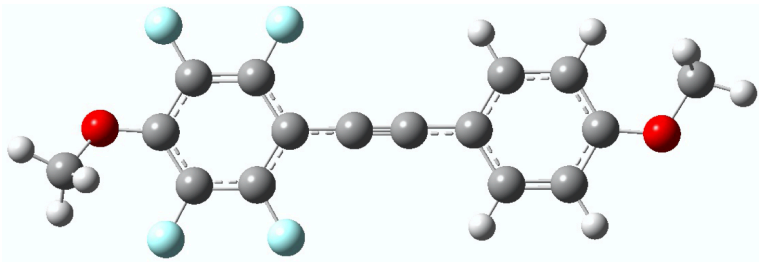

No.	Atom No.	Type	Coordinates (Angstroms) x	y	z
1	6	0	4.905300	0.963559	0.063238
2	6	0	3.513950	1.025009	0.044375
3	6	0	2.741717	-0.140929	-0.006507
4	6	0	3.394890	-1.387563	-0.038788
5	6	0	4.775858	-1.456747	-0.020466
6	6	0	5.540431	-0.281925	0.030783
7	1	0	5.475214	1.884285	0.103055
8	1	0	3.019332	1.991149	0.069542
9	1	0	2.804783	-2.297883	-0.078599
10	1	0	5.291601	-2.411339	-0.045178
11	6	0	1.313876	-0.068614	-0.025389
12	6	0	0.103251	-0.010262	-0.041785
13	6	0	-1.317154	0.056854	-0.059747
14	6	0	-2.108359	-1.093958	-0.070882
15	6	0	-1.999735	1.279561	-0.069452
16	6	0	-3.493510	-1.037817	-0.094455
17	6	0	-3.380287	1.344892	-0.078074
18	6	0	-4.167719	0.186694	-0.085079
19	8	0	6.884376	-0.453760	0.045312
20	6	0	7.701894	0.702261	0.097711
21	1	0	7.510835	1.276510	1.011146
22	1	0	8.729500	0.341263	0.101317
23	1	0	7.538717	1.337929	-0.779754
24	8	0	-5.501485	0.347122	-0.127261
25	6	0	-6.329450	-0.595600	0.565184
26	1	0	-5.876381	-0.869808	1.522137
27	1	0	-7.272579	-0.078169	0.736026
28	1	0	-6.494770	-1.486468	-0.042259
29	9	0	-3.981148	2.537112	-0.072990
30	9	0	-1.307501	2.420026	-0.056141
31	9	0	-1.527432	-2.295415	-0.077973
32	9	0	-4.179374	-2.189152	-0.149101

Dipole moment (field-independent basis, Debye):

X = 1.4062, Y = 0.0441, Z = 1.1135, Tot = 1.7942

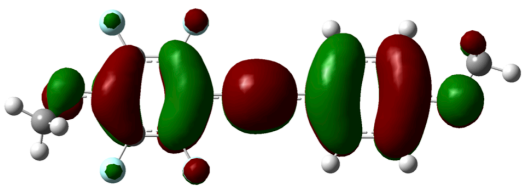

HOMO 79

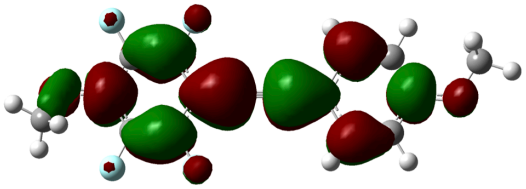

LUMO 80

Excited State 1: Singlet-A 4.2206 eV 293.76 nm *f*=1.4639 <S**2>=0.000

79 -> 80 0.68937

3-5. Geometry optimization for 2b

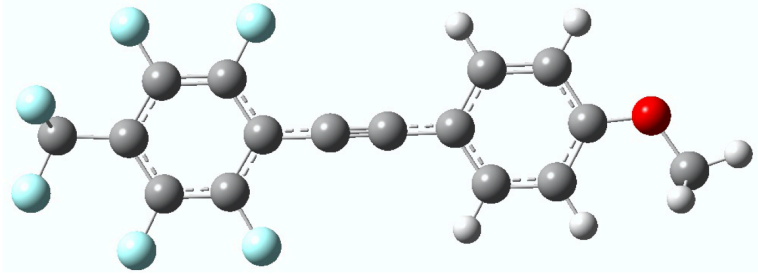

No.	Atom No.	Type	Coordinates (Angstroms) x	y	z
1	6	0	-5.349699	-1.423811	0.000012
2	6	0	-3.968716	-1.371136	0.000013
3	6	0	-3.303058	-0.130166	0.000005
4	6	0	-4.060782	1.046888	-0.000004
5	6	0	-5.451995	1.001599	-0.000005
6	6	0	-6.100689	-0.238219	0.000003
7	1	0	-5.876997	-2.372253	0.000019
8	1	0	-3.388152	-2.288370	0.000020
9	1	0	-3.554660	2.007327	-0.000010
10	1	0	-6.012307	1.928927	-0.000012
11	6	0	-1.876425	-0.075376	0.000007
12	6	0	-0.664713	-0.034075	0.000008
13	6	0	0.754631	0.004707	0.000003
14	6	0	1.515705	-1.170715	-0.000013
15	6	0	1.455294	1.213357	0.000015
16	6	0	2.897132	-1.127933	-0.000016
17	6	0	2.843144	1.257354	0.000013
18	6	0	3.590735	0.082552	-0.000003
19	8	0	-7.444233	-0.394291	0.000004
20	6	0	-8.251989	0.770874	-0.000004
21	1	0	-8.069136	1.373664	0.896323
22	1	0	-8.069136	1.373652	-0.896339
23	1	0	-9.282507	0.418715	-0.000001
24	6	0	5.098017	0.031646	-0.000007
25	9	0	5.553207	-0.623730	-1.079660
26	9	0	5.553211	-0.623759	1.079628
27	9	0	5.655352	1.243618	0.000009
28	9	0	3.576796	-2.275064	-0.000030
29	9	0	0.905488	-2.354103	-0.000025
30	9	0	0.784115	2.364019	0.000031
31	9	0	3.421522	2.456505	0.000026

Dipole moment (field-independent basis, Debye):

X = -6.3615, Y = 1.5252, Z = 0.0000, Tot = 6.5418

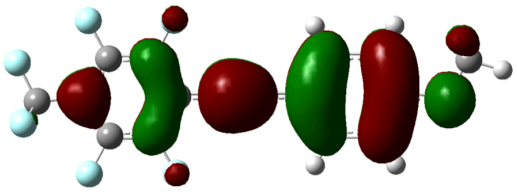

HOMO 87

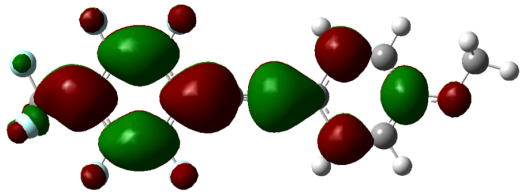

LUMO 88

Excited State 1: Singlet-A 4.0198 eV 308.44 nm *f*=1.3168 <S**2>=0.000

87 -> 88 0.68458

3-6. Geometry optimization for 2c

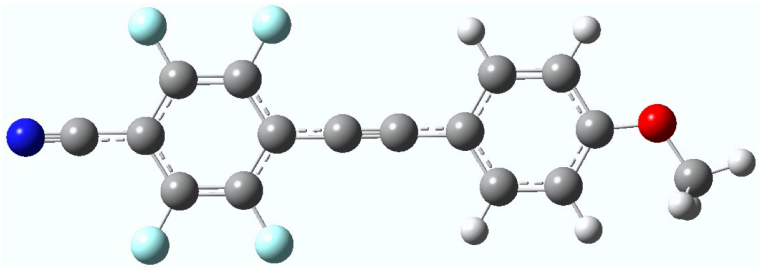

No.	Atom No.	Type	Coordinates (Angstroms) x	y	z
1	6	0	-4.654630	1.417642	0.000000
2	6	0	-3.273549	1.374183	0.000000
3	6	0	-2.600014	0.137231	0.000000
4	6	0	-3.349931	-1.045182	0.000000
5	6	0	-4.741067	-1.009011	-0.000001
6	6	0	-5.397803	0.226847	-0.000001
7	1	0	-5.188351	2.362455	0.000000
8	1	0	-2.698980	2.295168	0.000001
9	1	0	-2.837355	-2.002187	-0.000001
10	1	0	-5.295428	-1.939883	-0.000001
11	6	0	-1.173972	0.090474	0.000001
12	6	0	0.038291	0.053441	0.000001
13	6	0	1.456017	0.014367	0.000000
14	6	0	2.215426	1.191762	-0.000001
15	6	0	2.152146	-1.201479	0.000001
16	6	0	3.598088	1.157416	-0.000001
17	6	0	3.534712	-1.239972	0.000001
18	6	0	4.283268	-0.060220	0.000000
19	8	0	-6.741688	0.373988	0.000000
20	6	0	5.713120	-0.098242	-0.000001
21	7	0	6.869255	-0.129271	-0.000001
22	6	0	-7.542510	-0.796303	-0.000001
23	1	0	-7.355892	-1.397728	-0.896399
24	1	0	-7.355892	-1.397728	0.896397
25	1	0	-8.575044	-0.450239	-0.000001
26	9	0	1.600764	2.372440	-0.000001
27	9	0	4.279873	2.298254	-0.000002
28	9	0	1.476072	-2.348218	0.000002
29	9	0	4.155524	-2.415208	0.000002

Dipole moment (field-independent basis, Debye):

X = -8.4973, Y = -1.2970, Z = 0.0000, Tot = 8.5957

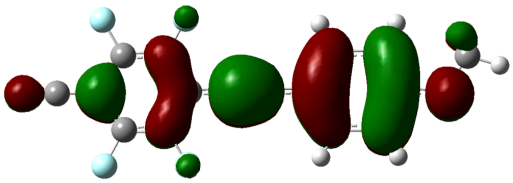

HOMO 77

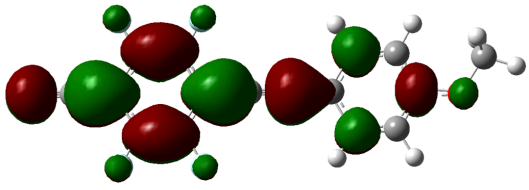

LUMO 78

Excited State 1: Singlet-A 3.8024 eV 326.07 nm *f* =1.4327 <S**2>=0.000

77 -> 78 0.68300

4. References

1 O. V. Dolomanov, L. J. Bourhis, R. J. Gildea, J. A. K. Howard and H. Puschmann, *J. Appl. Crystallogr.*, 2009, **42**, 339–341.

2 G. M. Sheldrick, *Acta Crystallogr. Sect. C Struct. Chem.*, 2015, **71**, 3–8.

3 M. J. Frisch, G. W. Trucks, H. B. Schlegel, G. E. Scuseria, M. A. Robb, J. R. Cheeseman, G. Scalmani, V. Barone, G. A. Petersson, H. Nakatsuji, X. Li, M. Caricato, A. V. Marenich, J. Bloino, B. G. Janesko, R. Gomperts, B. Mennucci, H. P. Hratchian, J. V. Ortiz, A. F. Izmaylov, J. L. Sonnenberg, D. Williams-Young, F. Ding, F. Lipparini, F. Egidi, J. Goings, B. Peng, A. Petrone, T. Henderson, D. Ranasinghe, V. G. Zakrzewski, J. Gao, N. Rega, G. Zheng, W. Liang, M. Hada, M. Ehara, K. Toyota, R. Fukuda, J. Hasegawa, M. Ishida, T. Nakajima, Y. Honda, O. Kitao, H. Nakai, T. Vreven, K. Throssell, J. A. Montgomery, Jr., J. E. Peralta, F. Ogliaro, M. J. Bearpark, J. J. Heyd, E. N. Brothers, K. N. Kudin, V. N. Staroverov, T. A. Keith, R. Kobayashi, J. Normand, K. Raghavachari, A. P. Rendell, J. C. Burant, S. S. Iyengar, J. Tomasi, M. Cossi, J. M. Millam, M. Klene, C. Adamo, R. Cammi, J. W. Ochterski, R. L. Martin, K. Morokuma, O. Farkas, J. B. Foresman and D. J. Fox, *Gaussian 16, Revision B. 01*; Gaussian, Inc., Wallingford, CT, USA, 2016.

4 (a) J. Andzelm, C. Kölmel and A. Klamt, *J. Chem. Phys.,* 1995, **103**, 9312; (b) V. Barone and M. Cossi, *J. Phys. Chem. A,* 1998, **102**, 1995; (c) M. Cossi, N. Rega, G. Scalmani and V. Barone, *J. Comput. Chem.,* 2003, **24**, 669.

5 (a) M. E. Vázquez, J. B. Blanco, B. Imperiali, *J. Am. Chem. Soc.* 2005, **127**, 1300; (b) M. Ravi, A. Samanta, T. Radhakrishnan, *J. Phys. Chem.* 1994, **98**, 9133; (c) H. Yao, T. Okada, N. Mataga, *J. Phys. Chem.* 1989, **93**, 738